الجمـهوريـة الجزائـريــة الديمقـراطيـة الشـعبيــة

REPUBLIQUE ALGERIENNE DEMOCRATIQUE ET POPULAIRE

وزارة التـعليم العالي والبـحـث العـلـمي

Ministère de l'Enseignement Supérieur et de la Recherche Scientifique

جـــامـعـة حـسيـــبة بـن بـوعـــلي – الشـــلـف

Université Hassiba Benbouali de Chlef (U.H.B.C)

Faculté de Technologie

Département d'Electrotechnique

Projet de Fin d'Etudes en vue de l'obtention du diplôme de

MASTER

Domaine : Sciences & Technologies

Filière : Electrotechnique

Option : Machines électriques

Présenté Par :

BOUKECIAT Bouchra

HIRECHE Sabrina

Thème

PID Gains-Based Super-Twisting control of a Synchronous Reluctance Machine

Soutenu le 24/06/2025, devant le jury composé de :

Président	Dr. BOUYAKOUB Ismail	MCA	Université de Chlef
Encadreur	Dr. BOUNADJA Elhadj	Professeur	Université de Chlef
Examinateur	Dr. TALEB Rachid	Professeur	Université de Chlef
Examinateur	Dr. BOUROUINA Ahmed	MCA	Université de Chlef

Année Universitaire : 2024/2025

ملخص: يُعد المحرك المتزامن ذوالممانعة (SynRM) آلة كهربائية تعمل بالتيار المتناوب، يتميز بالفعالية والصلابة، حيث يُنتج العزم من خلال تغير الممانعة المغناطيسية، دون الحاجة إلى ملفات على الجزء الدوّار أو إلى مغناطيسات دائمة. تهدف هذهالمذكرة إلى دراسة نمذجة هذا النوع من المحركات والتحكم المتقدم فيه، بهدف تحسين أدائه الديناميكي وزيادة قدرته على مقاومة الاضطرابات.وقد تم إجراء تحليل مفصل لبنية المحرك ونموذجه في الإطار الدوار d-q، حيث أظهر هذا التحليل وجود اقتران قوي بين التدفق المغناطيسي والعزم، مما يعقّد عملية التحكم ويجعل من الضروري استخدام استراتيجيات فصلمناسبة. في البداية، تم تطبيق تقنية التحكم المتجهي الموجه وفق تدفق الجزء الدوّار، وقد أظهرت نتائج مرضية تحت الظروف الاسمية، لكنها أظهرت تراجعًا في الأداء عند وجود تغيرات في معلمات المحرك.وللتغلب على هذه التحديات، تم اقتراح منظم يعتمد على خوارزمية **الانزلاق الفائق(Super-Twisting)** مع تعزيزها بمكاسب من نوع(PID)، ويُعرف باسم (**PID-STC**) يجمع هذا المتحكم بين الاستجابة الديناميكية السريعة، والقدرة العالية على مقاومة الاضطرابات، وتقليل ظاهرة التذبذب (chattering)وقد أثبتت نتائج المحاكاة فعاليته وتفوقه على المتحكمات التقليدية من نوع PI والمتحكم STC الكلاسيكي من حيث الدقة ورفض الاضطرابات.

Abstract: The Synchronous Reluctance Motor (SynRM) is a robust and efficient AC machine that generates torque through the variation of magnetic reluctance, without the need for rotor windings or permanent magnets. This Master's thesis investigates the modeling and advanced control of SynRMs to improve their dynamic performance and robustness. A detailed analysis of the motor's structure and its d-q frame model reveals strong flux–torque coupling, which complicates control and necessitates decoupling strategies. A rotor flux-oriented vector control approach is first implemented, yielding satisfactory results under nominal conditions but showing performance degradation under parameter variations. To address these limitations, a PID-based Super-Twisting Sliding Mode Controller (PID-STC) is proposed. This controller integrates robustness, fast dynamic response, and reduced chattering. Simulation results confirm its superiority over conventional PI and classical STC controllers in terms of precision and disturbance rejection.

Résumé : Le moteur synchrone à réluctance (SynRM) est une machine électrique robuste et efficace fonctionnant en courant alternatif, qui génère le couple par variation de la réluctance magnétique, sans recourir à des enroulements rotorique ni à des aimants permanents. Ce mémoire de master porte sur la modélisation et la commande avancée des moteurs SynRM, dans le but d'améliorer leurs performances dynamiques et leur robustesse. Une analyse détaillée de la structure du moteur ainsi que de son modèle dans le repère tournant ddd-qqq met en évidence un fort couplage entre le flux et le couple, ce qui complique la commande et nécessite des stratégies de découplage. Une approche de commande vectorielle orientée flux rotorique est d'abord mise en œuvre, donnant des résultats satisfaisants dans des conditions nominales, mais montrant une dégradation des performances en présence de variations des paramètres. Pour surmonter ces limitations, un contrôleur de type Super-Twisting basé sur la commande par mode glissant et enrichi de gains PID (PID-STC) est proposé. Ce régulateur offre une robustesse accrue, une réponse dynamique rapide et une réduction du chattering. Les résultats de simulation confirment sa supériorité par rapport aux régulateurs PI conventionnels et STC classique, en termes de précision et de rejet des perturbations.

ACKNOWLEDGMENTS

With God's help ,we hope to complete this work.

The work presented in this dissertation was carried out in the Electrical Engineering Department of the UHBB of Chlef.

We deeply thank Pr.El Hadj BOUNADJA, professor at the Electrical Engineering Department of the UHBB of Chlef, for supervising this dissertation. His scientific and human qualities have always been a source of motivation for us.

We sincerely thank the jury president for doing us the honor of chairing the defense jury. Our sincere thanks are also extended to the examiners for agreeing to examine this dissertation.

We would also like to express our gratitude to all the teachers in the Electrical Engineering Department of the UHBB of Chlef, particularly Dr. Mohamed BOUNADJA. We wish him good health and a successful return to his teaching work

Our sincere thanks also go to the people who helped us by contributing, directly or indirectly, to the completion of this work. May they find in this memoir a trace of our gratitude.

Dedication

To my parents with all my gratitude for all these

Years of sacrifice and encouragement

To myself and My cloud

To my family especially my sister

To those who shared my last year of study and this work with me “Sabrina”

To my friends

To all those I love

I dedicate this work

Thankyou for your encouragement and support.

BOUKECIAT Bouchra

Dedication

To my dear parents, with endless gratitude for their years of sacrifice, support, and unconditional love.

To myself,

For the resilience, growth, and perseverance through every challenge.

To my family,

The heart of my journey and the roots of my strength.

To my friends

To all those I love this work carries a part of you within it.

HIRECHE Sabrina

Table of contents

List of Figures

Chapter I: Mathematical modeling of the Synchronous Reluctance Motor (SynRM)

Chapter II: Field-Oriented Control of SynRM

Chapter III: PID Gain Based Super-Twisting control for a SynRM

Abbreviation	Full form
SynRM	Synchronous Reluctance Motor
SRM	Switched Reluctance Motor
IM	Induction Motor
ALA	AxiallyLaminatedAnisotropy
TLA	TransversallyLaminatedAnisotropy
SP	Salient Pole
Ns	Number of turns per phase (stator winding)
rs	Stator resistance per phase
Lls	Stator leakage inductance
Lmd	Direct-axis magnetizing inductance
Lmq	Quadrature-axis magnetizing inductance
Te	Electromagnetic torque
P	Number of poles
FOC	Field-Oriented Control
PI	Proportional-Integral
PWM	Pulse Width Modulation
d-axis	Direct axis (rotating reference frame)
q-axis	Quadrature axis (rotating reference frame)
vsd, vsq	d- and q-axis stator voltage components
isd, isq	d- and q-axis stator current components
ψsd, ψsq	d- and q-axis stator flux linkage

Abbreviation	**Full form**
Rs	Stator resistance
Ld, Lq	d- and q-axis inductances
Te	Electromagnetic torque
ωe	Electricalangular speed
ωr	Mechanicalangular speed
TL	Load torque
J	Moment of inertia
β	Friction coefficient
MTPA	Maximum Torque per Ampere
s	Laplace operator (complexfrequency)
Vd, Vq	d- and q-axis voltage control inputs
Id, Iq	d- and q-axis current
SMC	Sliding Mode Control
STA	Super-Twisting Algorithm
PID	Proportional-Integral-Derivative
MLI	Modulation Largeur Impulsion
PWM	Pulse Width Modulation
FOC	Field-Oriented Control

List of Symbols

1. Electrical Quantities (Stator Reference Frame)

vsd,vsq_	Stator voltage components in d- and q-axis
isd,isq	Stator current components in d- and q-axis
ψsd,ψsq	Stator flux linkage components in d- and q-axis
Rs	Stator resistance
Ld,Lq	Direct and quadrature axis inductances

2. Electrical Quantities (Rotor Reference Frame)

id,iq	d-axis and q-axis currents in the rotor reference frame
vd,vq	d-axis and q-axis voltages
ωr	Rotor angularvelocity
θ	Rotor position angle

3. Machine and MechanicalParameters

Te	Electromagnetic torque
ω_e	Electricalangularvelocity
ωr	Mechanical angular velocity (sometimes rotor angular velocity)
TL	Load torque
J	Moment of inertia

β	Friction coefficient

4. Inductances and Resistances (Detailed Parameters)

r_s	Stator resistance per phase
L_{ls}	Stator leakage inductance
L_{md}	Direct-axis magnetizing inductance
L_{mq}	Quadrature-axis magnetizing inductance

5. Controller Parameters

Kp	Proportional gain (PI controller)
Ki	Integral gain (PI controller)
Ur	Controller output
$\epsilon(t)$	Error signal in time domain

6. MathematicalOperators and Variables

S	Laplace operator (complex frequency variable)
d\dt	Time derivative operator (used in differential equations)

7. Machine Structural Parameters

P	Number of pole pairs or Number of poles (check context)

General Introduction

1- Motivation and Context:

In recent years, the global shift toward energy-efficient, cost-effective, and sustainable technologies has fueled the widespread adoption of electric drives across diverse sectors, including industrial automation, electric mobility, and renewable energy systems [1], [2]. Among the various types of electrical machines, the Synchronous Reluctance Motor (SynRM) has emerged as a promising solution due to its simple and robust construction, absence of rotor windings or permanent magnets, and high efficiency [3], [4]. These advantages make SynRMs especially attractive for medium- and high-performance applications, where both reliability and cost-effectiveness are essential [5].

Despite its structural and thermal advantages, the SynRM poses significant challenges in terms of control. Its operation is governed by inherently nonlinear and strongly coupled dynamics, particularly between the flux and torque components [6]. This makes precise and stable control difficult to achieve, especially in the presence of parameter uncertainties and external disturbances such as load torque variations or changes in supply conditions [7]. Traditional Proportional-Integral (PI) controllers, although widely used in vector-controlled drive systems, often fail to provide the required performance in such demanding scenarios due to their limited robustness and slow transient response [8].

To address these limitations, Sliding Mode Control (SMC) techniques have gained popularity for their inherent robustness to matched disturbances and modeling inaccuracies [9]. In particular, the Super-Twisting Control (STC), a second-order SMC method, offers advantages such as continuous control action, finite-time convergence, and mitigation of the chattering effect typical of first-order sliding modes [10], [11]. However, even STC may show limited responsiveness under rapid transients or highly dynamic reference tracking tasks [12].

.

2- Objective of the Thesis

This thesis proposes an enhanced sliding mode speed controller based on the Super-Twisting Control, ameliorated with a derivative action on the sliding variable. The proposed controller—referred to as PID gains-based Super-Twisting Control (PID-STC)—aims to improve the system's dynamic response while preserving robustness to model uncertainties and external

perturbations. The inclusion of a derivative term in the sliding mode control law provides anticipatory action during fast transients, thereby enhancing performances of the system.

3- Structure of the Thesis

To validate the proposed approach, the thesis is structured into three chapters:

- *Chapter 1 – Mathematical Modeling of the Synchronous Reluctance Motor (SynRM):* This chapter presents a detailed modeling of the SynRM, including its historical background, physical construction, and magnetic characteristics. The motor is modeled in the d-q rotating reference frame, which forms the foundation for control design. The coupling between torque and flux is discussed, and the control challenges associated with SynRM dynamics are highlighted.
- *Chapter 2 – Vector Control Applied to the Synchronous Reluctance Motor**:*** This chapter investigates the implementation of stator flux-oriented vector control, aimed at decoupling flux and torque. The classical PI-based control strategy is discussed in terms of performance under nominal and non-nominal conditions. The limitations of this method in handling parameter variations and external disturbances are analyzed, motivating the use of more robust nonlinear controllers.
- *Chapter 3 – PID Gains-Based Super-Twisting control of a Synchronous Reluctance Motor:*

  The final chapter introduces the proposed PID-STC control approach. After presenting the theoretical foundations of the standard STC, the modified version with derivative enhancement is developed. The controller is tested on a MATLAB/Simulink model of the SynRM. Comparative simulation results with traditional PI and classical STC controllers are presented, focusing on key performance indicators such as speed tracking, settling time, overshoot, and robustness under disturbances.

Chapter I:
Mathematical modeling of the Synchronous Reluctance Motor (SynRM)

I.1.Introduction

Synchronous reluctance machines (SynRM) are a type of electric motor that generate moyion and torque using the principle of magnetic reluctance. Unlike traditional motors with permanent magnets, SynRM-similar to switched reluctance machines (SRM)-operate without magnets and are powered by sinusoidal currents that produce a rotating magnetic field. They feature a durable construction, with a stator similar to that of an induction motor and a magnet-free, copper-free rotor. This simple and efficient design makes SynRM a promising low-cost solution for a variety of applications [13].

I.2.History of the development of (SynRM)

The development of synchronous reluctance motors (SynRM) dates back to the 1930, when researchers explored ″unexcited salient pole synchronous motors‟-early versions of variable reluctance synchronous machines-for applications requiring precise, constant-speed operation and self-starting capability. However, their adoption was limited due to low efficiency and poor power factor [14][15].

Interest resurfaced in the 1960, especially in the UK, where innovations like segmented rotors, flux barriers, and axially laminated designs aimed to boost the saliency ratio and overall performance. Meanwhile, in France, the attention for its high torque density and suitability for low-speed direct drive systems.

The term ‟switched reluctance motor″ was coined in 1969, and by the 1990, electronically controlled double-saliency machines began gaining momentum in both academia and industry. Companies like allenwest Ltd. (UK) and Sicme-motori(Italy) ere among the first to commercialize thes designs.

In recent years,SynRM have gaines renewed attention for their simple construction, high efficiency, low production cost, and reliable operation. Despite these advantages, challenges such as noise reduction and further efficiency improvements continue to drive research in design and control strategies. Today, SynRM are used in divers applications including the textilleindustry, machine tools, high-speed machinery, electric vehicles, pumps, and ventilation systems[16][17].

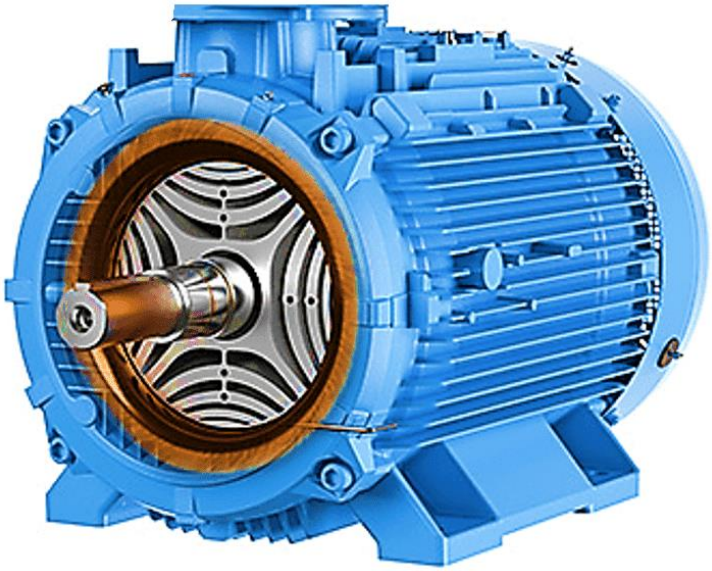

Figure I.1: Sunchronous reluctance motor.

I.3.Construction

I.3.1 Stator

The synchronous reluctane motor (SynRM) utilise the same stator as the induction motor (IM), consisting of electrical steel sheets configured in a tooth-slot geometry (see figure I.2). This geometry is formed by punching the steel sheets using a specialized tool. Once shaped, the sheets are stacked, electromagnetically insulated from one another, and compressed to create a solid lamination stack.

Stator windings are then inserted into the slots along the stator's inner circumference. Typically, a three-phase winding is employed. Although multiphase SynRM variants exist, they fall outside the scope of this thesis. The windings are sinusoidallydistriputed, and when supplied with the appropriate current, generate a rotating circular magnetic field in the air gap. Consequently, the magnetic induction within the air gap closely approximates a sinusoidal waveform-acknowledging that no real motor achieves perfect ideality. In most designs, the SynRM stator is implemented without skewing.

This means that SynRM stators can be manufactured using the same existing assembly lines as induction motors (IM), greatly simplifying and facilitating their mass production [18].

FigureI.2: stator of SynRM

I.3.2 Rotor

the rotor of synchronous reluctance motor must have salient poles to generate variable reluctance within the motor's angular position. These salient poles are typically formed by milling axial slots along the length of a squirel cage rotor. The rotor includes multiple pairs of slots, which can be positioned either on the outer surface or internally.

The outer slots are formed along the rotor's outer periphery, while the inner slots are positioned within the interior of the rotor. The distance from the rotor's outer edge to the outer slot is set to be 0.7 to 1.3 time the width of the stator's magnetic pole. The total magnetic flux of the outer permanent magnent, placed in the outer slot, is designed to be equal to or greatervthan that of the inner permanent magnent located in the inner slot. To assemble the rotor, a process called explosion bonding is used. This method employs explosive energy to press multiple metal sheets together under extremely high pressure, causing several atomic layers at the contact surfaces to momentarily behave like a fluide, therby forming a solid-state bond.

The angle at whichethe two metals collide during explosion bonding causes thfluide-like metal interface to jet outward, effectively cleaning the surfaces. This ultra-clean interface, combined with the high pressure forcing the metal sheets together, creates optimal conditions for solid-state welding. Exprimental tests on a stainless steel and mild steel bond have showthat the resulting tensile and fatigue strengths exceed those of theindividual base materials, primarily due to shock hardening that occurs during the process. Furthermore, the bond was tested 20°C to 70°C, showing no significant loss in tensile strength. The explosion bonding process is illustrated in fig(I.3). In addition to this technique, other methods such as brazing, roll bonding, or diffusion bonding may also be suitable for rotor construction.

Initially, sheets of ferromagnetic and non-magnetic steel are bonded together, as illustrated in fig (I.3). These bonded sheets are then cut into rectangular blocks, which are subsequently machined into shaft can also be machined from the same block, allowing for an integrated rotor and shaft assembly[18].

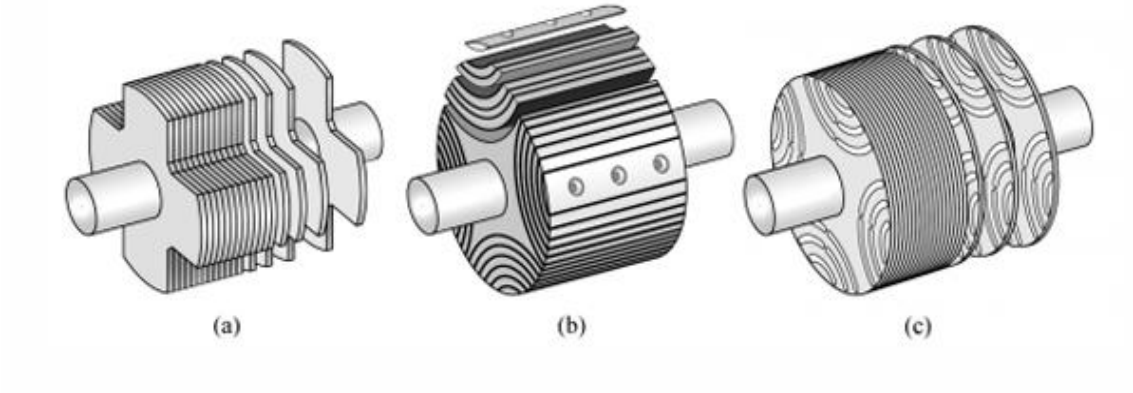

FigureI.3: Possible rotor design for a SynRM: (a) Simple salient pole (SP) rotor, (b) Axially laminated anisotropy (ALA) rotor, (c) Transversally laminated anisotropic (TLA) rotor.

I.4.Working principale of synchronous reluctance motor

The stator of this motor features a single main winding, which alon cannot produce a rotating magnetic field. To achieve this, at leat two windings separated by a specific phase angle are required. Therefore, an additional winding called the auxiliary winding is included in the stator.

Thois auxiliary winding is connected in series with a capacitor to create the necessary phase shift for generating a rotating magnetic field.

A phase difference exists between the current-carrying winding and their corresponding magnetic fluxes. These two fluxes interact to produce a rotating magnetic field, a process known as the split-phase method.

The speed of the magnetic field, known as synchronous speed, is determined by the number of poles in the stator winding. The rotor contains copper or aluminum bars that are short-circuited, functioning similary to the squirel-cage rotor found in induction motors.

When in iron object is placed in a magnetic field, it naturally aligns with the path of least magnetic reluctance, becoming magnetically locked. Similarly, the rotor in a reluctance motor attempts to align with the axis of the rotating magnetic field at the position of least reluctance. However, this alignment cannot occur when the rotor is stationary due its initial inertia.

The rotor in the motor initoally accelerates toward synchronous speed, operating similary to a squirel-cage induction motor. Once it reaches synchronous speed, the stator's magnetic field pulls the rotor into the position of least magnetic reluctance, locking it magnetically. From that point on, the rotor continues to rolate at synchronous speed.

Reluctance torque is the torque produced due to the rotor's tendency to align with the position of least magnetic reluctance. As a result, the reluctance motor ultimately operates like a synchronous motors .for this to happen effectively, the rotor resistance should be low, and combined inertia of the rotor and load must also be minimal[19].

I.5.Mathemetical model of SynRM

I.5.1.The d-q equation of SynRM

A 2-pole synchronous reluctance motor is shown in Figure I.4. It features a 3-phase stator winding and a salient-pole rotor. The stator windings are identical, each having Nsequivalent turns and resistance rs, and are spaced 120° electrical degrees apart. It is typically assumed that the windings are sinusoidally distributed. Due to this sinusoidal distribution, the flux harmonics in the air gap contribute only an additional component to the stator leakage inductance, without significantly impacting the fundamental air-gap flux.

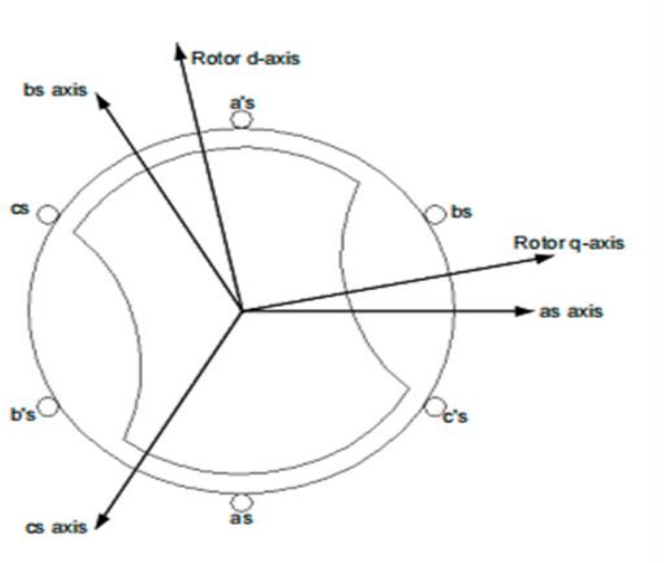

FigureI.4: two-pole Synchronous reluctance motor.

This additional term affects only the stator leakage inductance. As a result, the dynamic behavior of a synchronous reluctance machine can be derived from the conventional equations of a wound-field synchronous machine. However, unlike traditional machines, the synchronous reluctance motor (SynRM) lacks an excitation (field) winding. Furthermore, in modern SynRM designs typically incorporating axially or transversely laminated rotor structures a rotor cage is also absent. This is because the machine can start synchronously from zero speed when driven by a properly controlled inverter. Consequently, by removing the field and damper winding components from Park's equations, the fundamental **d-q axis equations** governing the operation of a synchronous reluctance machine can be obtained. Specifically, these equations are[20]:

$$\begin{cases} \text{vd} = r_s i_{ds} + \frac{d\lambda_{ds}}{dt} - \omega_r \lambda_{\alpha s} \\ vq = r_s i_s + d\frac{\lambda_{qs}}{dt} + \omega_r \lambda_{ds} \end{cases} \quad \text{(I.1)}$$

Where

$$\begin{cases} \lambda_{d_s} = l_{k_s} i_{d_s} + l_{m_d} i_{d_s} = l_{d_s} i_{d_s} \\ \lambda_{q_s} = l_{k_s} i_{q_t} + l_{m_q} i_{a_s} = l_{q_p} i_{a_s} \end{cases} \quad \text{(I.2)}$$

Here,l_{i_s},l_{m_d} and l_{m_q}represent the stator leakage inductance, direct-axis magnetizing inductance, and quadrature-axis magnetizing inductance, respectively. The parameter Rsdenotes the stator resistance per phase. When expressed in terms of the d-q reference frame variables, the electromagnetic torque expression remains the same as that of a conventional synchronous machine, and is given by:

$$Te = \frac{3}{2}\frac{p}{2}(\lambda_{ds} i_{\psi s} - \lambda_{as} i_{ds}) \tag{I.3}$$

Where P is the number of poles.

I.5.2.The study state equation for a synchronous reluctance motor:

The d-q equations describe the behavior of the stator and rotor currents in a reference frame that rotates with the rotor similar to the rotor reference frame used in wound-field synchronous machines. When balanced three-phase voltages are applied to the stator, they produce a constant-magnitude rotating voltage vector in the d-q plane. If the rotor rotates at the same angular velocity as this voltage vector (adjusted by the number of pole pairs), the voltage vector appears stationary in the rotor reference frame. Under these conditions, it is customary to define the angular relationship between the stator voltage vector and the d-q axes using two components, as illustrated in Figure I.5:

$$\begin{cases} V_{q_s} = \grave{V_s} \cos\delta \\ V_{d_s} = -\grave{V_s} \sin\delta \end{cases} \tag{I.4}$$

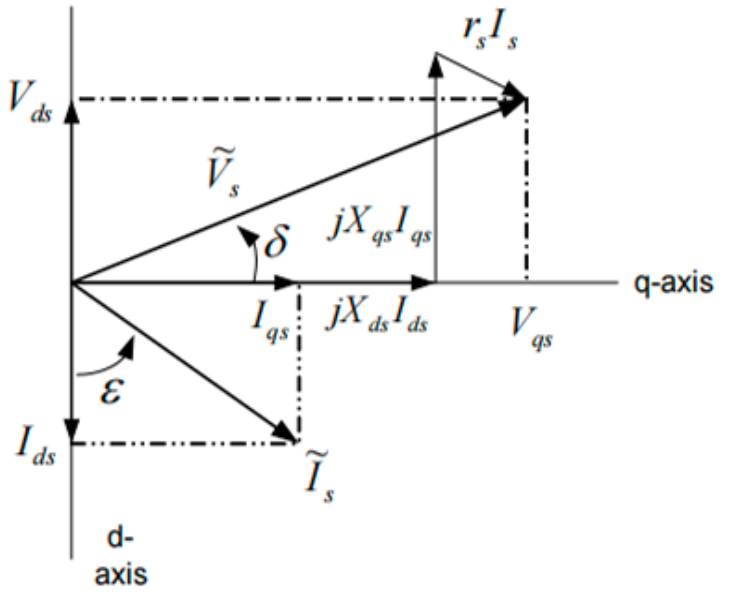

FigureI.5**:**phasor diagram for synchronous reluctance machine.

The "variables" in the differential equation (I.1) also become constant in steady state. That is the d dt terms can be eliminated. The currents can then be solved in terms of the steady state voltages as[20]:

$$\begin{cases} I_{d_s} = \frac{w_e l_{q_s} V_{q_s} + r_s V_{d_s}}{r_s{}^2 + w_e{}^2 l_{d_s} l_{q_s}} \\ I_{q_s} = \frac{-w_e l_{d_s} V_{d_s} + r_s V_{q_s}}{r_s{}^2 + w_e{}^2 l_{d_s} l_{q_s}} \end{cases} \quad \text{(I.5)}$$

Or :approximately, neglecting stator resistance as:

$$I_{ds} = \frac{V_{qs}}{W_e L_d}, I_{qs} = \frac{-V_{ds}}{W_e L_{qs}} \quad \text{(I.6)}$$

I.5.3.Phasor Equation for a Synchronous reluctance machine:

Alternatively, we can create a signalephasor equation from the study state version of (I.1) by multiplying the first line of (4.1) by –j and adding it to the second line. The result is:

$$V_{qs} - jV_{ds} = rs(I_{qs} - jI_{ds}) + w_e(\lambda_{ds} + j\lambda_{qs}) \quad \text{(I.7)}$$

Or :using (I.2) and (I.7)

$$V_{qs} - jV_{ds} = r_s\,(I_{qs} - jI_{ds}) + w_e(L_{ds}I_{ds} + jL_{qs}I_{qs}) \quad \text{(I.8)}$$

(I.8) can be manipulated to the fromof:

$$V_{qs} - jV_{dt} = rs(I_{as} - jI_{ds}) + jw_eL_{ds}(-jI_d) + jw_eL_{qs}I_{qs} \quad \text{(I.9)}$$

In phasornotation :

$$V`_s = r_s\grave{I}_s + jX_{ds}\grave{I}_{ds} + jX_{qs}\grave{I}_{qs} \quad \text{(I.10)}$$

Alternatively, the results of (I.5) can be obtaind from this phasor equation. A phasor diagram is show in figure (I.5) [20].

I.6.Advantages of Synchronous Reluctance Motors

Synchronous reluctance motors (SynRM) offer several advantages, making them a robust and efficient choice for many applications[21]:

- The machine maintains a constant speed under all operating conditions due to its magnetic locking principle. By producing synchronized torque, it effectively handles load variations whether underloaded or overloaded while keeping the speed stable.
- Unlike conventional synchronous motors, which are not self-starting and require a starting mechanism, this machine self-starts thanks to the reluctance principle. This contributes to its enhanced durability and simpler design, resulting in reduced maintenance requirements.
- Additionally, unlike switched reluctance motors, it does not suffer from torque ripple, leading to smoother operation.
- One of the key advantages of using synchronous motors is the ability to control the power factor. An over-excited synchronous motor, which operates with a leading power factor, can be used in parallel with induction motors and other lagging power factor loads to improve the overall system power factor.
- Synchronous motors can be designed with wider air gaps compared to induction motors, enhancing mechanical stability. Moreover, the electromagnetic power developed in a synchronous motor varies linearly with the applied voltage.

- Synchronous motors also typically achieve higher efficiency often exceeding 90% especially in low-speed and unity power factor applications.
- Notably, this machine does not require a DC supply for excitation, simplifying its construction and further reducing maintenance needs.
- For high-quality synchronous reluctance motors that offer reliable performance without the need for continuous maintenance, consider reaching out to Epoch Automation Pvt. Ltd.

I.7.Disadvantages of synchronous reluctance motor|[22]

- The power factor is lower in comparison to that of permanent magnet synchronous machines.
- It exhibits lower efficiency relative to high-end permanent magnet machines.
- Exhibits lower torque density relative to machines utilizing magnets or windings.
- Susceptible to higher levels of noise and vibration due to saliency-induced effects.
- Produces lower starting torque than induction motors unless specifically optimized.
- Dynamic performance is limited in the absence of control systems.
- Control strategies are required to maintain synchronization under varying load conditions.

I.8.Application of Synchronous reluctance motors [18]

- It is popularly used in many low power applications such as fiber spinning mills because of inherent simplicity, robustness of construction and low cost.
- Widely used for many constant speed applications such as recording instruments, timing devices, control apparatus and phonograph.
- Used as proportioning devices in pumps or conveyors.
- Applied in auxiliary time mechanism.
- Used in processing of continuous sheet or film material.
- Used in regulators and turntables.
- Applied in wrapping and folding machines.

- It can be used in synchronized conveyors.
- In metering pumps also, the synchronous reluctance motor is used.
- Used in synthetic fibre manufacturing equipment.

I.9. Numerical Simulation of the SynRM powered by a perfectly grid

Numerical simulation allows for precise modeling, analysis, and evaluation of electrical systems. Today, a wide range of software tools is available for the simulation of electrical machines. For the purpose of simulating the Synchronous Reluctance Motor (SynRM), MATLAB/Simulink was selected due to its robustness and versatility.

The studied machine—whose parameters are detailed in Appendix A—is a Synchronous Reluctance Motor (SynRM) powered by a perfectly sinusoidal three-phase grid.

Figure I.4 illustrates the performance of the SynRM during no-load startup. It can be observed that the stator currents are significantly high, which may cause thermal stress and potentially damage the machine if such start-ups are repeated frequently. During the transient phase, the electromagnetic torque exhibits strong oscillations, which can result in audible noise from the mechanical components. After the transient phase, which lasts approximately 0.7 seconds, the machine reaches nearly synchronous speed (157 rad/s), given the absence of load (negligible slip). The electromagnetic torque stabilizes after a brief period to compensate for frictional losses under no-load conditions, while the rotor flux reaches a steady-state value of 1.5 Wb.

Following the no-load operation, a mechanical load torque of 5 Nm is applied between t=1 s. It is observed that the electromagnetic torque stabilizes around 5 Nm, and the rotor speed drops to approximately 147 rad/s, close to the nominal value. The quadrature and direct rotor flux components are significantly affected, indicating a strong coupling between torque and speed on one hand, and between torque and stator flux on the other.

Additionally, the stator three-phase current remains sinusoidal and balanced, but its amplitude increases during the loaded condition, reflecting the additional power demand required driving the applied torque.

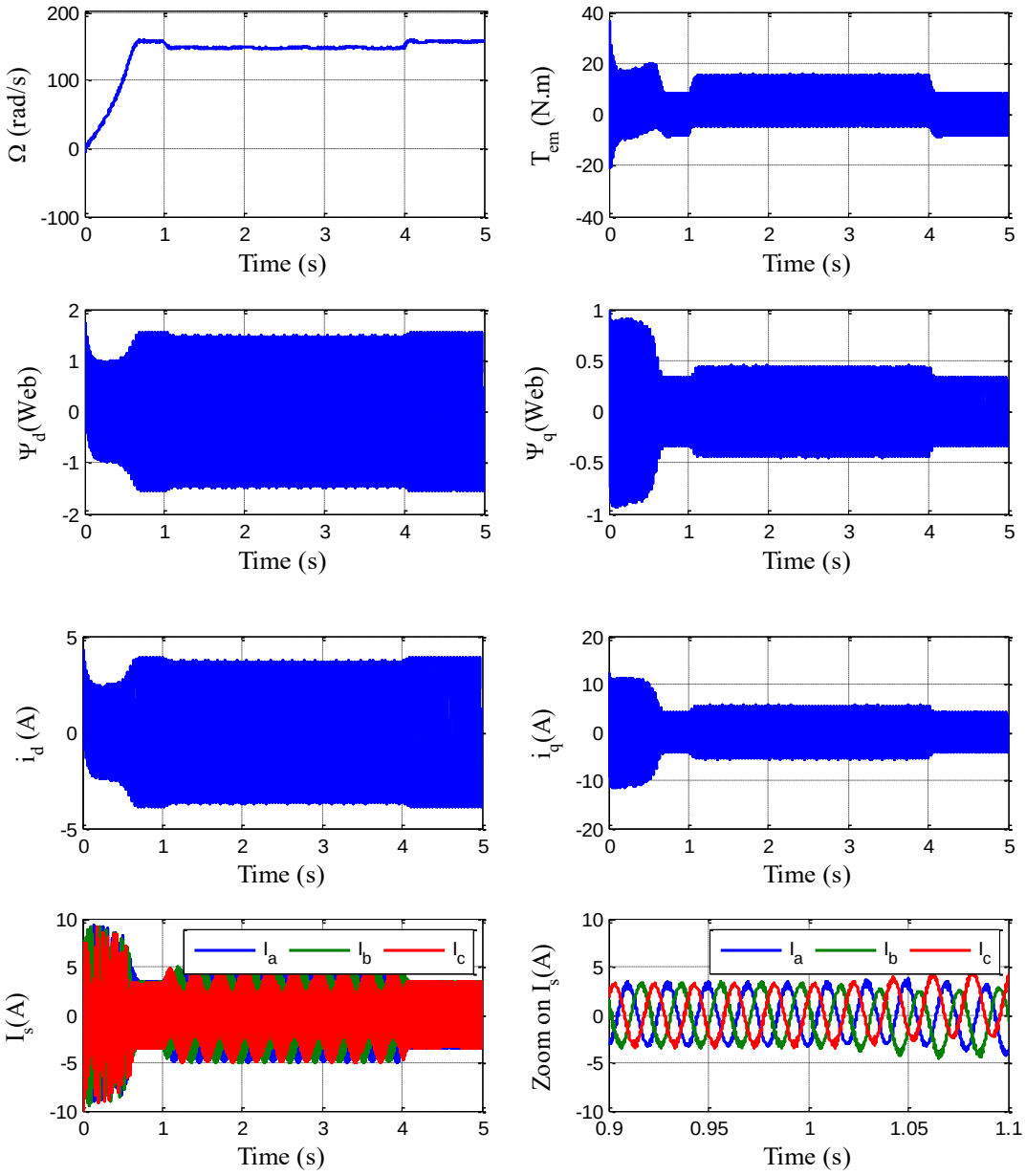

Figure I.6: Performance of the SynRMDuring a No-Load Start-Up Followed by the Application of a Load Torque Cr=5 Nm Between 1 s and 4 s.

I.10.Conclusion:

In summary, this chapter has laid the theoretical and physical foundations necessary for the effective control of Synchronous Reluctance Motors (SynRMs). Beginning with an overview of their historical development and growing significance in modern electric drive systems, the chapter explored the motor's physical structure and the mechanism of torque generation via magnetic reluctance. The mathematical modeling of the SynRM in the ddd–qqq rotating

reference frame was established, forming the basis for the design of advanced control strategies addressed in subsequent chapters.

Furthermore, the simulation results presented at the end of this chapter—based on a SynRM powered by a perfectly balanced grid—clearly reveal a strong coupling between the flux and torque components. This intrinsic coupling significantly complicates control and necessitates the implementation of decoupling strategies to achieve precise and independent regulation of torque and flux. Finally, the discussion highlighted key control challenges, including nonlinearities, parameter sensitivity, and torque ripple, thereby justifying the use of robust and sophisticated control algorithms for optimal SynRM performance.

Chapter II:
Field-Oriented Control of the Synchronous Reluctance Motor (SynRM)

II.1.Introduction

High-performance electric drive systems are now designed to fulfill the main requirements, such as fast transients, high power density, high efficiency, and low rotor inertia.

On a large scale, the most popular electric machine is the induction one, but it has low efficiency and a low power range, which makes it inappropriate for this kind of application.

A secondary option is represented by the permanent magnet synchronous machine, with various benefits such as high efficiency and low rotor inertia, but with the main drawback of the demagnetization phenomenon when operating at high temperatures. At last, the synchronous reluctance machine (SynRM) becomes an attractive solution for a large range of power and speed, being a low-cost machine with eco-friendly environmental impact and multiple benefits, such as compact sizes, low mass and rotor inertia, and the rotor having no electric windings, cage, or permanent magnets. For the modern applications of SynRM drives, advanced control algorithms are used to obtain high performances such as fast transient regimes, good tracking results, and efficient disturbance rejection [23][24].

For the efficient control of alternating current machines, their modeling is based on the *dq*0 transformation [25][26], which generates *dq*axes models. The main control strategies of SynRM based on the *dq* axes model are divided into the following categories [27][28]: constant *d*- axis current control (when the torque is varied by the *q*-axis current), current angle control (with the groups: fast torque response, maximum power factor control, maximum torque per ampere control), and active flux control. These control strategies are usually implemented using the field-oriented control (FOC) concept, which involves a cascade control structure with an outer loop for angular speed control and an inner loop for *d*-axis and *q*-axis current control.

II.2. MODELLING OF SYNCHRONOUS RELUCTANCE MOTOR

Space vector theory is a powerful mathematical tool used to analyze and control electric machines. Itinvolves the representation of three-phase quantities such as voltages, currents, and magnetic fluxes as two-dimensional vectors in a complex plane as shown in Figure 1. This transformation simplifies the analysis ofthree-phase systems by converting them into a single vector in the d-q plane (direct-quadrature plane), whichcorresponds to a rotating reference frame aligned with the rotor's magnetic field.

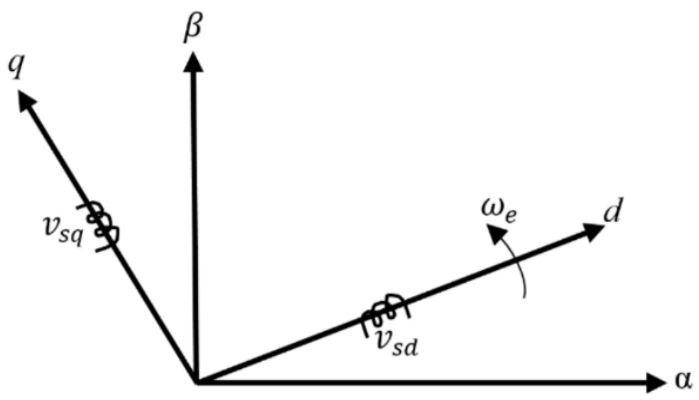

Figure II.1: Circuit representation of SynRM

In this study, the Synchronous Reluctance Motor (SynRM) model is developed based on the following simplifying assumptions:

- Sinusoidal Stator Winding Distribution**:** The stator windings are assumed to be sinusoidally distributed, allowing for the use of fundamental harmonic analysis and simplifying the derivation of the electromagnetic equations.

- Linear Magnetic Circuit**:** The magnetic circuit is considered linear, implying that magnetic saturation effects are neglected. This assumptionfacilitatesanalyticalmodeling by ensuring constant inductances.

- Rotor without Damper Bars: The rotor is assumed to have no damper windings or bars, which eliminates rotor-induced currents and simplifies the dynamic model.

  The motor's space vector model in the synchronously rotating reference frame, which rotates at an electrical angular speed of , is presented as follows [29][30].

II.2.1.Voltage Equations

$$v_{sd} = i_{sd}R_s + \frac{d\psi_{sd}}{dt} - \omega_e\psi_{sq} \quad \text{(II.1)}$$

$$v_{sq} = i_{sq}R_s + \frac{d\psi_{sq}}{dt} + \omega_e\psi_{sd} \quad \text{(II.2)}$$

Where vsd and vsq are the d- and q-axis components of the stator voltage vector, Rs is the stator resistance, isd and isq are the d- and q-axis components of stator current vector, ψsd and ψsq are the d- and q-axis components of the flux linkage

II.2.2.Flux Linkage Equations

The stator flux linkage vector ψs is related to the stator current vector is via the stator inductances. For a Synchronous Reluctance Motor (SynRM), the d-q axis components of the flux linkage can be expressed as:

$$\psi_{sd} = i_{sd} L_{sd} \tag{II.3}$$

$$\psi_{sq} = i_{sq} L_{sq} \tag{II.4}$$

Where:

- Ψsd_ψsq are the d-axis and q-axis components of the stator flux linkage,
- Isd_isq are the corresponding components of the stator current,
- Ld_ Lq are the direct- and quadrature-axis inductances of the motor.

II.2.3.Electromagnetic Torque Equation:

The electromagnetic torque generated by the motor, together with its mechanical-dynamic equation of motion, can be expressed as:

$$T_e = \frac{3}{2} P (L_{sd} - L_{sq}) i_{sd} i_{sq} \tag{II.5}$$

$$T_e - \beta \omega_r - T_L = J \frac{d\omega_r}{dt} \tag{II.6}$$

where, ωr represents the angular mechanical speed, P is the number of pole pairs, TL is the mechanical load torque, and J is the moment of inertia, β denotes the friction coefficient. The torque equation can also be expressed as follows:

$$T_e = \frac{3}{2} P (\psi_{sd} i_{sq} - \psi_{sq} i_{sq}) \tag{II.7}$$

II.3.FIELD-ORIENTED CONTROL STRATEGY OF SynRM

In FOC, the stator currents are decoupled into d-axis (direct) and q-axis (quadrature) components, enabling independent control of magnetic flux and torque similar to a separately excited DC motor. The FOC strategy lings the stator flux vector with the d-axis (ψ_{sq}=0). From equation (3), it is evident that the direct-axis flux is directly regulated by the d-axis stator currenti_{ds}.By substituting ψ_{sq}= 0 in equation (7), it will be simplified to

$$T_e = \frac{3}{2}P(\psi_{sd} i_{sq}) \tag{II.8}$$

The working principal of FOC is to decouple the stator currents into their flux- and torque-producing components (i_d andi_q, respectively). Consequently this strategy guarantees separated control of the flux and torque of the machine.[31],[32].

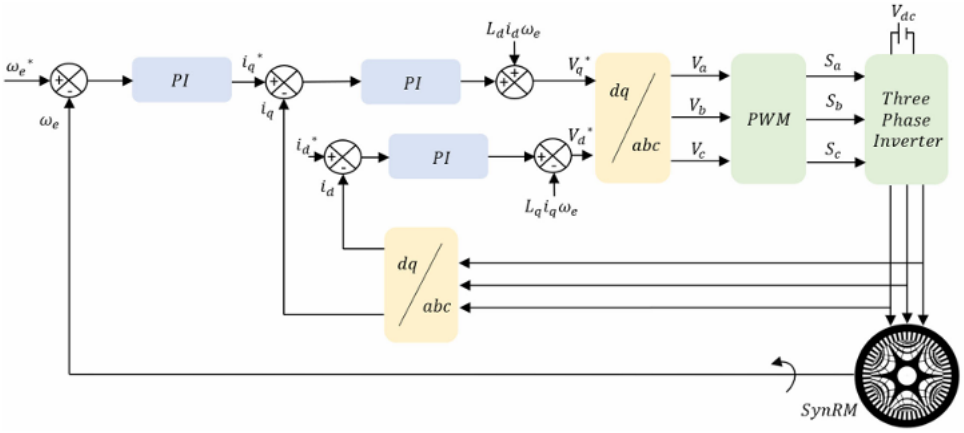

Figure II.2: The field-oriented control of SynRM

As shown in Fig.1 Three control loops are used to ensure precise regulation of speed and torque. The process begins with the speed loop, where the reference speed ωe∗ is compared to the actual speed ωe. The resulting error is processed by a proportional-integral (PI) controller, which outputs the reference torque-producing current iq∗. This current enters the q-axis current loop, where it is compared with the measured iq. The error is again regulated using a PI controller to produce the reference voltage vq∗, with an added dynamic compensation term related to the cross-coupling effects. Simultaneously, the d-axis current loop regulates the magnetic flux,

usually by setting id∗=0, which maximizes torque production in SynRM. The computed reference voltages vd∗andvq∗are then transformed into three-phase voltages via inverse Park transformation (dq → abc), and sent to a PWM generator to control a three-phase inverter. Finally, the phase currents are measured and transformed into idandiq components, closing the control loops and enabling dynamic and efficient motor operation.

II.3.1.Principle of Field-Oriented Control

Field-Oriented Control (FOC) is widely recognized in the field of motor control due to its excellent steady-state behavior, maintaining its relevance despite the emergence of newer techniques. Its strong appeal lies in its ability to deliver accurate torque regulation, low torque ripple, and a constant switching frequency, which are essential in demanding industrial applications such as mining and steel production [33].

FOC operates by transforming the motor equations into a rotating reference frame (d–q frame), which allows for the decoupling of torque and flux components. This transformation simplifies control, making the AC motor behave similarly to a DC motor from a control perspective.

II.3.2.Advantages of FOC:

- Excellent Stenay-state performance,
- Précise curent control,
- Relative y simple implementation,
- Compatibility with various AC motor types,
- Simplified modulation process,
- Fixed switching frequency.

However, these benefits come with certain limitations. FOC systems are computationally intensive due to their reliance on PI controllers and Pulse-Width Modulation (PWM) techniques, which can introduce delays and affect dynamic response. Additionally, since torque control is achieved indirectly, the system may exhibit slower reactions to load or reference changes. Moreover, the method is sensitive to parameter variations, which can degrade performance.

II.3.3.Limitations of FOC:

- High processing requirements due to its control and modulation strategies,
- Reduced dynamic response because of indirect torque regulation,
- Sensitivity to motor parameter variations, limiting robustness.

II.4.Decoupled Control Strategy and Control Loops in FOC

Subsequently, from Equation (8), it becomes evident that maintaining a constant stator flux allows for the linear control of the electromagnetic torque through the quadrature-axis component of the stator current, isq. This indicates that the Field-Oriented Control (FOC) strategy successfully achieves decoupled control of flux and torque (or speed).

II.4.1.Control Objective: Flux and Torque Decoupling

Objective of Flux and Torque decoupling:

The goal is to control flux (id) and torque (iq) independently, which allows:

- Enhanced dynamic response
- More precise torque control
- Higher energy efficiency

II.4.2.Advanteges of Decoupled Control:

- Faster and more stable torque respose
- Better efficiency using MTPA (Maximum Torque per Ampere)strategy
- Reduced torque ripple
- Makes use of a robust, magnet-free motor design.

II.4.3.Control System Structure: Inner Current Loop and Outer Speed Loop

The FOC system consists of:

- **Inner Current Loop**: This fast loop controls the d-and q-axis currents, ensuring rapid response to current commands.

- **Outer Speed Loop**: This slower loop regulates the motor speed by generating the appropriate torque reference for the inner loop.

For the outer loop, meant to control the angular speed of SynRM, the PI controller is the most frequently used [27][34].

II.5.DecouplingTechnique:

II.5.1.MathematicalRepresentationofCoupling

The vector control laws for machines supplied with voltage exhibit coupling between the controls actions on the d- and q-axes. In a rotating reference frame (d,q), with the d-axis aligned with the rotor flux, the machine's behavior can be described by the following equations [35]:

$$\begin{cases} V_d = \left(R_s I_d + L_d \frac{dI_d}{dt}\right) - \omega L_q I_q \\ V_q = \left(R_s I_q + L_q \frac{dI_q}{dt}\right) + \omega (L_d I_d) \end{cases} \quad \text{(II.9)}$$

$with: \ \omega = P.\omega_r$

$$\begin{cases} V_d = (R_s + L_d.s) I_d - \omega L_q I_q \\ V_q = \left(R_s + L_q.s\right) I_q + \omega (L_d I_d) \end{cases} \quad \text{(II.10)}$$

S: Laplace operator.

Figure (II.3) illustrates the coupling between the d- and q-axes:

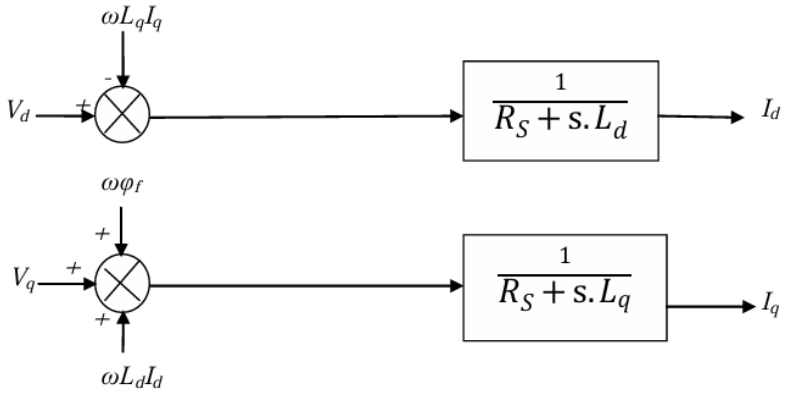

Figure II.3: Description of the couplings.

This coupling is eliminated by a compensation method, which consists of adding specific terms to make the d- and q-axes completely independent.

II.5.2.DecouplingbyCompensation

The purpose of compensation is to decouple the d- and q-axes. This decoupling simplifies the expression of both the machine equations and the control structure, making it easier to compute the regulator gains [36].The principle of this decoupling is to define two new control variables, as illustrated in Figure (II.4) Such that:

$$\begin{cases} V_d = V*_d - e_d \\ V_q = V*_q - e_q \end{cases} \tag{II.11}$$

$$\begin{cases} V*_d = L_d \frac{dI_d}{dt} + R_s I_d \\ V*_q = L_q \frac{dI_q}{dt} + R_s I_q \end{cases} \tag{II.12}$$

With:

$$\begin{cases} e_d = \omega L_q I_q \\ e_q = 0 \end{cases} \tag{II.13}$$

As a result, the currents are decoupled: the current iddepends only on vd, and iqdepends only on v*q. Based on equation (II.12), the currents can be expressed as follows:

$$\begin{cases} I_d = \frac{V*_d}{R_s - S.L_d} \\ I_q = \frac{V*_q}{R_s - S.L_q} \end{cases} \tag{II.14}$$

The control principle involves regulating the stator currents based on the reference values (desired set points) using conventional controllers such as PI regulators .As a result, the control actions along the direct (d) and quadrature (q) axes are decoupled, allowing independent regulation of flux and torque-producing components.

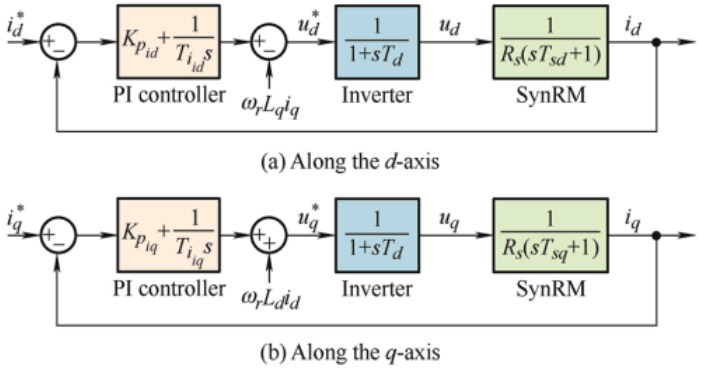

Figure II.4: Decoupled Control Structure for d-q Axis Regulation

II.6.RegulatorDesign

When the decoupling between the d-axis and the q-axis is achieved and **Id** is kept at zero,

II.6.1.PI Controller Design

The role of controllers is to maintain the output variable equal to the imposed reference value, despite the presence of internal or external disturbances [36]. Once decoupling between the d-axis and q-axis is achieved, regulation is performed using proportional-integral (PI) controllers. The integral action serves to minimize the error between the reference and the regulated quantity, while the proportional action adjusts the system's response speed [36]. The PI controller combines both proportional and integral actions in parallel,

The relationship between the output u(t) and the error signal e(t) is given by the following expression:

$$U_r = K_p \varepsilon(t) + K_i \int_0^t \varepsilon(t)_{dt} \tag{II.15}$$

That is to say:

$$\frac{U_{(s)}}{\varepsilon_{(t)}} = K_p + \frac{k_i}{s} \tag{II.16}$$

With:

K_p: Proportional gain

K_i: Integral gain

The PI controller is represented by the following figure:

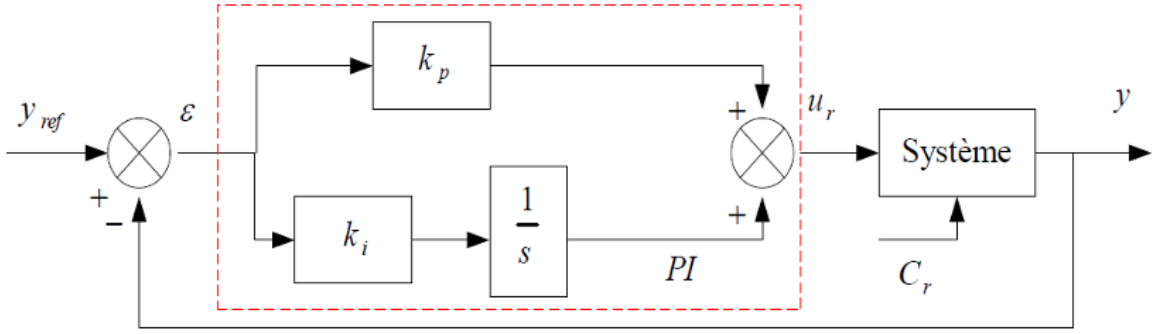

Figure II.5: PI Controller

The transfer function of the PI controller is given by:

$$\frac{U_r}{\epsilon} = k_p + \frac{k_i}{s} \tag{II.17}$$

The PI controller can also be expressed in the following form

$$P.I \rightarrow \frac{U_r}{\epsilon} = \frac{1+ST_1}{ST_2} \tag{II.18}$$

With:

$$\begin{cases} K_p = \frac{T_1}{T_2} \\ K_i = \frac{1}{T_2} \end{cases} \tag{II.19}$$

II.6.2.PI Controller Tuning

II.6.2.1. Regulation of the q-axis Current (i_q)

Based on the relationships derived from Equations (II.14) and (II.18), the regulation loop for the q-axis current is illustrated in Figure (II.6).

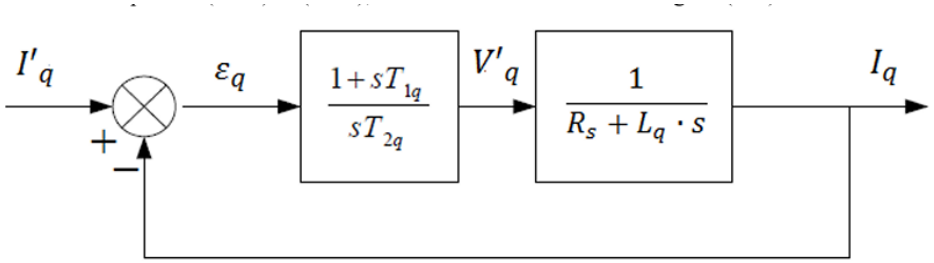

Figure II.6: coil for controlling the current q

This diagram represents the control structure for iq using a Proportional-Integral (PI) controller in an open-loop configuration. The design of the controller relies on the pole compensation method, which aims to achieve a well-balanced dynamic response.

The key objective is to align the time constant of the PI controller with the electrical time constant of the q-axis, ensuring stability and responsiveness.

Following this design strategy, a closed-loop transfer function is obtained, which characterizes the overall system behavior under control. It demonstrates how the PI controller improves system performance by minimizing dynamic error and enhancing current regulation efficiency.

II.6.2.2 Regulation of the d-axis Current (i_d)

The regulation loop for the d-axis current is shown in Figure (II.7).

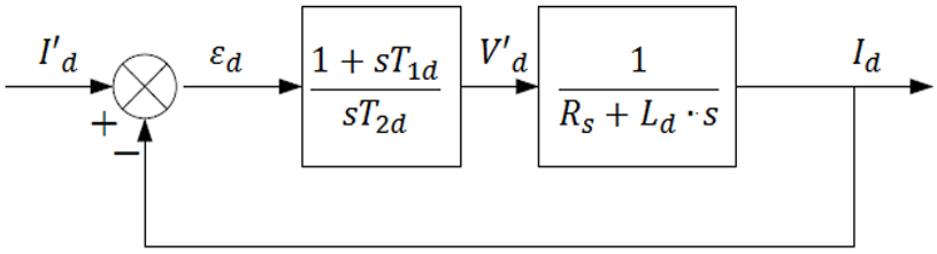

Figure II.7:coil for controlling the current.

To control the d-axis current, the same methodology used for the regulation of the q-axis current is applied. This includes designing a Proportional-Integral (PI) controller based on pole compensation to ensure effective and stable current regulation.

As in the q-axis case, the open-loop transfer function is derived, and the electrical parameters of the d-axis are taken into account. By substituting the relevant expressions, the closed-loop

transfer function is then obtained. This function describes the dynamic behavior of the system when regulating the d-axis current and highlights the effectiveness of the PI controller in minimizing steady-state error and improving the system's dynamic performance.

II.6.2.3. Speed Regulation

The system to be controlled is divided into two subsystems:

- The current regulation subsystem, which also controls the electromagnetic torque,
- The mechanicalsubsystem.

In this model, the mechanical constant of the machine is considered. The closed-loop transfer function (FTBF) of the system is derived and analyzed to understand the system’s dynamic behavior.

After simplifications and approximations, the characteristic polynomial of the transfer function is obtained, revealing that the system behaves like a second-order dynamic system. This allows the system to be represented in a canonical second-order form characterized by its natural frequency and damping factor.

II.7. Simulation results

The performance of the flux-oriented control was tested through numerical simulation. The simulations were carried out on a SynRM whose parameters are provided in Appendix A. Figure 3.15 shows the Simulink model of the vector control used for the closed-loop speed regulation of the SynRM.

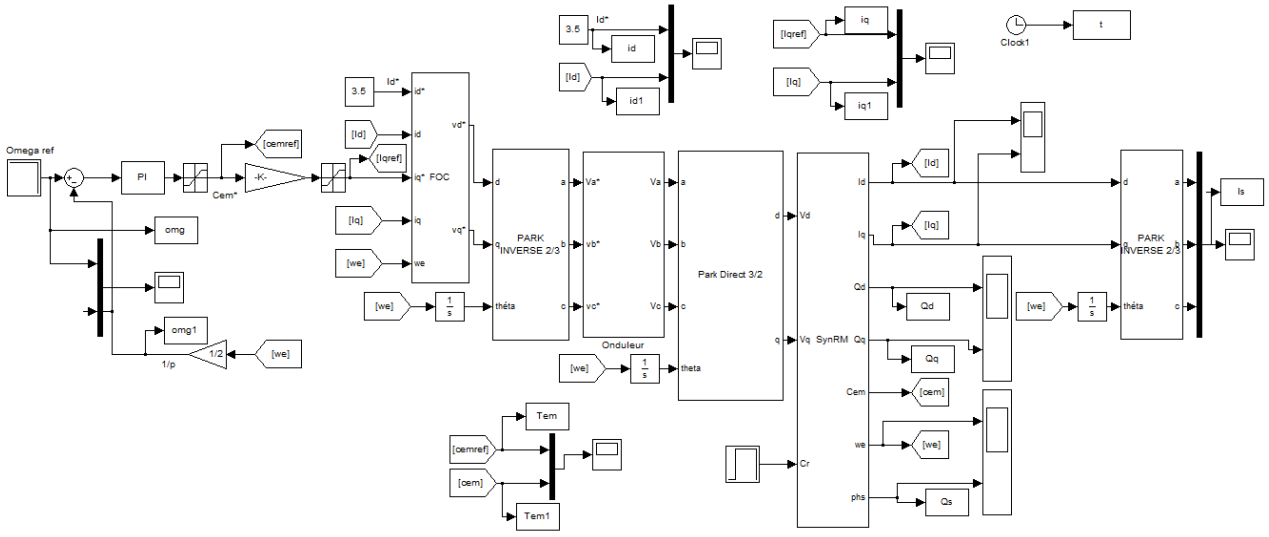

Figure II.8: Simulink model of the vector control of the SynRM.

II.7.1. Reference tracking test

The performance of the proposed vector control strategy for the speed regulation of the Synchronous Reluctance Motor (SynRM) was evaluated through numerical simulations. The test scenario involved a speed step of 100 rad/s, including a reversal of the rotation direction at t = 2.5 s. Additionally, a load disturbance of 15 N·m was applied between t = 1 s and t = 4 s.

Figures 3.17 to 3.20 illustrate the simulation results obtained using a PI controller with stator current limitation. The key observations are summarizedbelow:

- Speed Tracking (Ω) : The rotor speed closely follows the reference profile, confirming accurate tracking throughout the test. A temporary speed drop is observed when the 15 N·m load torque is applied at t = 1 s; however, the system rapidly returns to the desired speed.
- Electromagnetic Torque Response (Tem): A peak is observed at startup, followed by stabilization at the expected value, indicating effective torque generation and control.
- Direct-Axis Current (I_d): The direct-axis current remains close to zero during operation, validating the effectiveness of the decoupling strategy implemented in the vector control scheme.

- Quadrature-Axis Current (I_q): The quadrature current accurately reflects the torque demand, confirming that the electromagnetic torque is primarily governed by this current component.
- **Stator Phase Currents**: The real (phase) stator currents exhibit a sinusoidal waveform, indicating proper functioning of the inverter and confirming that the vector control strategy generates balanced and low-distortion current profiles.

Despite the overall satisfactory performance, the *Id* and *Iq* currents exhibit pronounced transients (overcurrents) during dynamic phases such as startup and load application. These overcurrents can result in high line currents, potentially stressing or damaging the inverter's semiconductor devices. To address this, a limitation on the stator currents has been incorporated into the control strategy.

In this condition, the simulation results confirm that the vector control of the SynRM ensures **stable**, **accurate**, and **good** performance in terms of both speed and torque, while offering a fast dynamic response to load variations and maintaining sinusoidal phase currents for improved power quality.

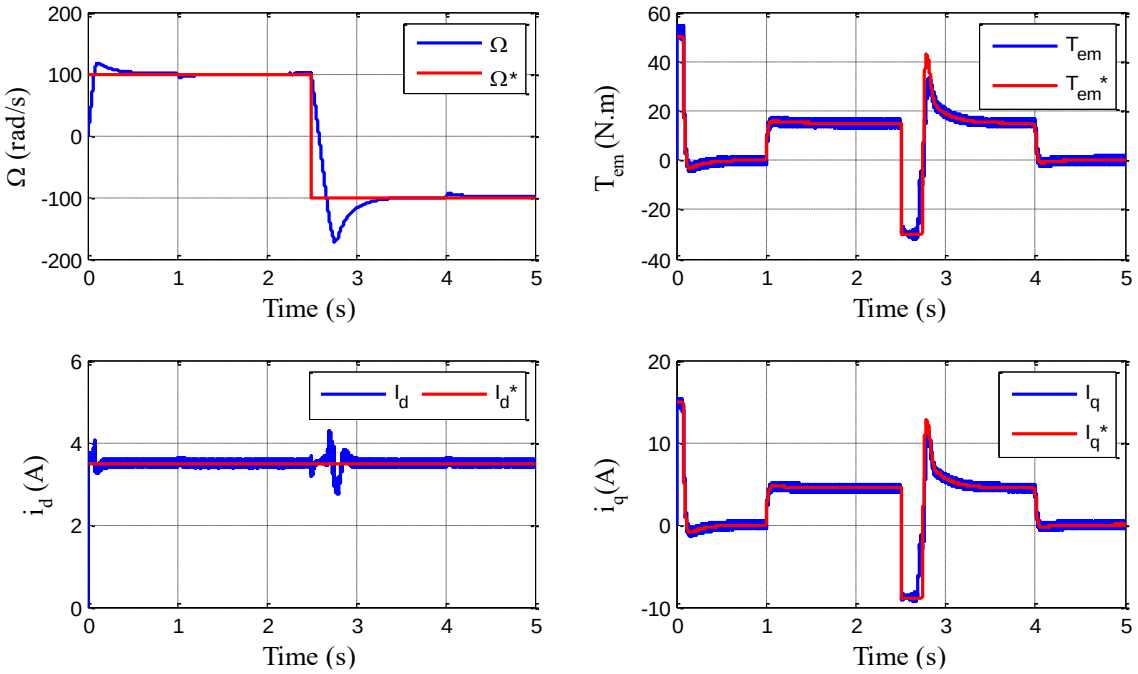

Figure III.9 : Speed regulation (with PI controller) of the SynRM using vector control for a reference speed of $\pm 100\,rd/s$, with load disturbance of 15 N·m was applied between t = 1 s and t = 4 s.

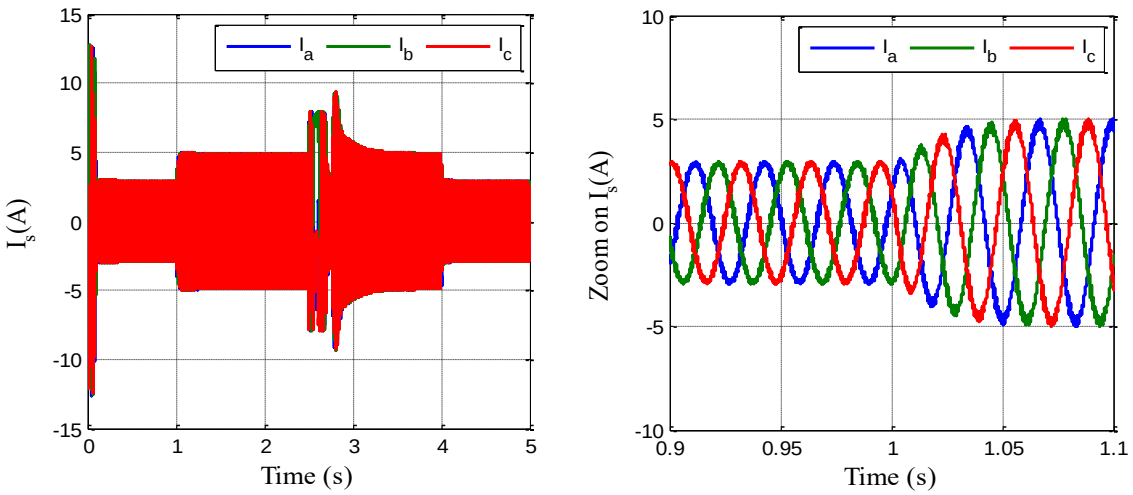

Figure III.10 : Three Phase Stator Currents of the SynRM using vector control for a reference speed of $\pm 100\, rd/s$, with load disturbance of 15 N·m was applied between t = 1 s and t = 4 s.

II.7.2. Robustness Analysis under Parametric uncertainty

In practice, the parametric identification of an electrical machine does not provide perfectly accurate or constant values. The machine parameters—such as stator resistance, inductances, and moment of inertia—are subject to variation due to operating conditions like temperature rise, load changes, magnetic saturation, air gap geometry, skin effect, or field weakening. Therefore, it is important to investigate how deviations from nominal parameters affect the control performance, particularly in terms of speed and rotor flux regulation.

To simulate this behavior, the machine model is intentionally subjected to parameter variations at a specific time, while the control algorithm continues to operate using the nominal parameters. The machine is controlled via indirect vector control based on rotor flux orientation and operates under nominal load. A conventional PI controller is used for speed regulation.

The robustness of the control strategy is evaluated under the following parameter perturbations (as shown in Figure III.22):

- A +100% increase in the stator resistance Rs,
- A 100% reduction in both direct and quadrature inductances Ld and L,
- A +100% increase in the moment of inertia J.

Speed Response:

Despite significant parameter mismatches, the rotor speed remains not well regulated. A notable effect is a slight increase in the speed response time and a significant overshoot observed during startup and reversal of rotation. These deviations reflect the system's reduced dynamic performance under mismatched inertia, but they do not critically affect steady-state tracking.

Electromagnetic Torque:

The electromagnetic torque, however, fails to accurately track its reference during transients and steady- state. This discrepancy is particularly visible during acceleration and deceleration phases. It indicates a sensitivity of the torque loop to parameter variations, highlighting the limitations of the PI controller when it relies on inaccurate machine models.

Flux Components:

The two stator flux components remain effectively decoupled throughout the test, even under the introduced disturbances. This confirms that the field-oriented control structure maintains its core decoupling principle, though its dynamic performance is slightly degraded.

Three-Phase Stator Currents:

The three-phase stator currents maintain a balanced and sinusoidal waveform, which ensures good power quality and inverter operation. However**,** the amplitude of the currents increasesnoticeably due to the rise in stator resistance, which leads to higher copper losses and increased thermal stress on the machine and the inverter. This highlights the importance of current limitation mechanisms when dealing with parameter uncertainty.

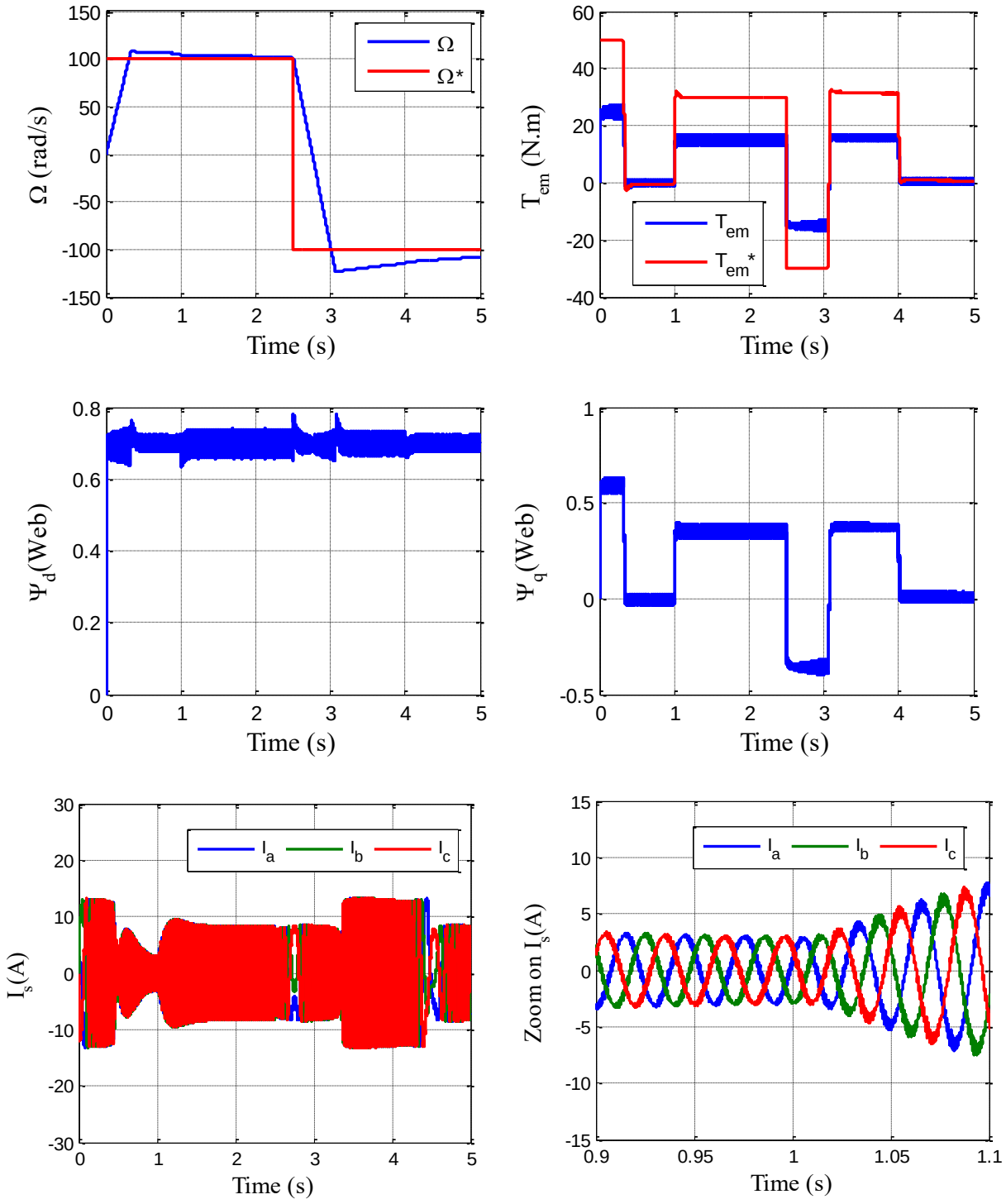

Figure III.11: robustness test for speed control of SynRM(under nominal load)using vector control.

II.8.Conclusion

This chapter has examined the application of flux-orientedcontrol to the Synchronous Reluctance Machine (SynRM), highlighting its ability to decouple stator flux and electromagnetic torque. As a result, the SynRM achieves dynamic performance comparable to that of a separately excited DC machine. By this method the decoupling is well achieved under nominal conditions.

Simulation results confirm that under ideal conditions, the vector control strategy provides accurate speed tracking, effective flux decoupling, and sinusoidal stator current profiles. However, the system's performance can degrade when subjected to parameter uncertainties such as increased stator resistance, reduced inductances, and higher inertia.

In such cases, although speed regulation remains acceptable, the electromagnetic torque fails to follow its reference precisely, especially during transients. Moreover, an increase in stator resistance results in higher current amplitudes, leading to increased power losses and thermal stress on the drive components. These issues underline the importance of robust control techniques and current limitation mechanisms.

To address these limitations, the next chapter explores advanced sliding mode control as a means of enhancing the SynRM’s performance and robustness under uncertain conditions and external disturbances.

.

Chapter III: PID Gains-Based Super-Twisting control of a Synchronous Reluctance Motor

III.1 Introduction

The control of alternating current (AC) machines, including the Synchronous Reluctance Motor (SynRM), presents significant challenges due to the strong coupling between the flux and torque components, which introduces a degree of nonlinearity in the system model. This complexity has motivated the development of advanced control strategies that aim to emulate the decoupled nature of DC motors, where flux and torque can be controlled independently [37].

Sliding Mode Control (SMC), especially in its classical first-order form, has been widely used due to its robustness against parameter variations (internal uncertainties) and external disturbances such as load torque variations. Classical SMC is typically applied to systems with a relative degree of one, where the control input appears in the first derivative of the sliding surface [38].

In the case of SynRM, SMC is particularly appealing due to its ability to handle the model uncertainties arising from rotor saliency and magnetic saturation, both of which are characteristic of this motor type. Additionally, it provides a fast dynamic response, which is essential for high-performance applications.

However, one of the major drawbacks of classical SMC is the chattering phenomenon—undesired high-frequency switching of the control signal. This effect can excite unmodeled dynamics, leading to system degradation, mechanical stress, and even potential instability or damage.

To overcome this limitation, Higher-Order Sliding Mode Control (HOSMC) has been introduced, with the Super-Twisting Algorithm (STA) and Twisting Algorithm being two well-known second-order implementations. These techniques reduce or eliminate chattering while preserving robustness. Among them, the Super-Twisting Algorithm is particularly effective for systems with relative degree one and continuous outputs, making it a strong candidate for SynRM speed control.

Furthermore, recent improvements in the STA include gain adaptation using PID principles, resulting in a PID-Gain-Based Super-Twisting Sliding Mode Controller (PID-STSMC). Thisvariant allows dynamic adjustment of control gains based on the tracking error, its derivative, and integral, offering enhanced performance, reduced chattering**, and** improved transient behavior**.**

This chapter introduces the general concepts of **variable structure systems** and the design principles behind both first-order and second-order sliding mode controllers**,** analyzed in thephase plane**.** We present the mathematical formulation, control synthesis steps, and application of both techniques to SynRM speed control**.** The chapter concludes with a **c**omparative study between the twisting and PID-based Super-Twisting controller**s**, evaluating their performance in terms of robustness, convergence speed, and chattering suppression.

III.2 First-Order Sliding Mode Control (SMC)

III.2.1 Variable Structure Systems in Sliding Mode

A Variable Structure System (VSS**)** is a system whose dynamics change during operation based on a defined switching logic**.** This concept is central to Sliding Mode Control (SMC**),** which provides strong robustness properties, especially useful when applied to systems with uncertain or varying parameters. In the case of Synchronous Reluctance Motors(SynRM)**,** this control strategy is particularly effective in dealing with parameter uncertainties, such as those arising from the machine's anisotropic magnetic structure **and** load disturbances**.**

The core idea is to design a sliding surface (typically a hyperplane in the state-space) toward which the system state trajectories are driven. Once this surface is reached, a switching control law ensures that the system remains in its vicinity, producing a robust behavior that is insensitive to matched perturbations. For SynRM drives, this facilitates accurate torque and speed **control,** even under nonlinear or varying conditions.

The system trajectory in the phase plane typically consists of three distinct modes, each corresponding to a different stage in the regulation process [38].

III.2.2 Trajectory Modes in the Phase Plane

III.2.2.1 Reaching Mode (RM)

In this initial phase, the controlled variable (e.g., motor speed) moves from any initial state toward the switching surface defined by**S(x) = 0**, within a finite time**.** The design of the control law and the application of a convergence criterion (such as Lyapunov-based stability conditions) ensure this transition. For SynRM systems, this mode is essential **for** quick transient response during start-up or command changes [37].

III.2.2.2 Sliding Mode (SM)

Once the system state reaches the sliding surface, it enters the sliding mode. Here, the system's behavior is governed only by the dynamics on the sliding surface, which is immune to matched disturbances and parameter variations. For the SynRM, this allows for **stable and robust speed control,** even in the presence of disturbances such as mechanical load fluctuations or magnetic saturation.

III.2.2.3 Steady-State Mode (SSM)

This mode examines the system's behavior around the equilibrium point, typically at the origin of the phase plane. It characterizes the system's steady-state accuracy and performance, which is critical in nonlinear systems. For SynRM drives, a well-behaved steady-state mode ensures precise and stable operation, which is vital for high-performance industrial applications requiring speed and torque consistency **[**37**]**.

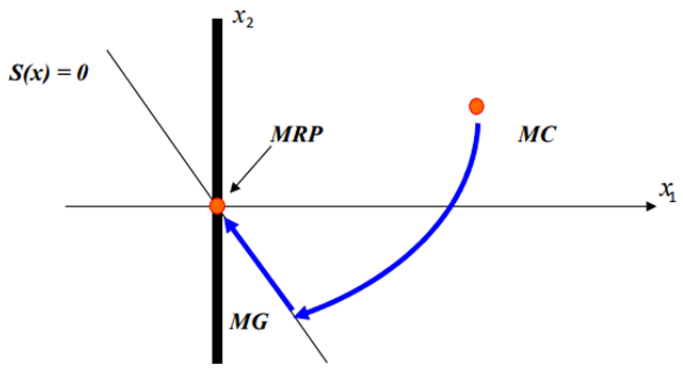

Figure III.1: Different Modes of the Trajectory in the Phase Plane

III.2.3 Ideal and Real Sliding Regimes

In theory, the switching mechanism in a sliding mode controller is considered perfectly robust against noise, allowing the system trajectory to precisely follow the sliding surface, typically defined by the condition S(x)= 0. This is referred to as **t**he ideal sliding regime, where the system's representative point slides exactly along the switching hyper surface.

In the ideal case, this sliding motion is characterized by an infinite switching frequency and zero amplitude oscillations**,** which implies perfect tracking and instantaneous response. For a Synchronous Reluctance Motor (SynRM**),** such ideal behavior would result in extremely

accurate torque and speed regulation**,** even in the presence of disturbances or model uncertainties.

However, in practice, the implementation of such high-frequency switching is not feasible due to:

- Physical limitations of power electronics (e.g., switching losses, finite bandwidth),
- Measurement noise affecting feedback signals,
- And modeled system dynamics (e.g., parasitic inductances or delays).

As a result, the real sliding regime exhibits small-amplitude oscillations around the sliding surface—a phenomenon known as chattering**.** In the case of SynRM drives, chattering can lead to undesirable effects such as mechanical vibrations**,** additional energy losses**,** and evenwear on actuators**.**

To mitigate this, advanced techniques such as higher-order sliding mode control (e.g., Super-Twisting Algorithm) or continuousapproximations of the switching function are employed. These modifications allow the controller to maintain robustness while reducing or eliminating chattering, thereby ensuring smooth and stable operation of the SynRM.

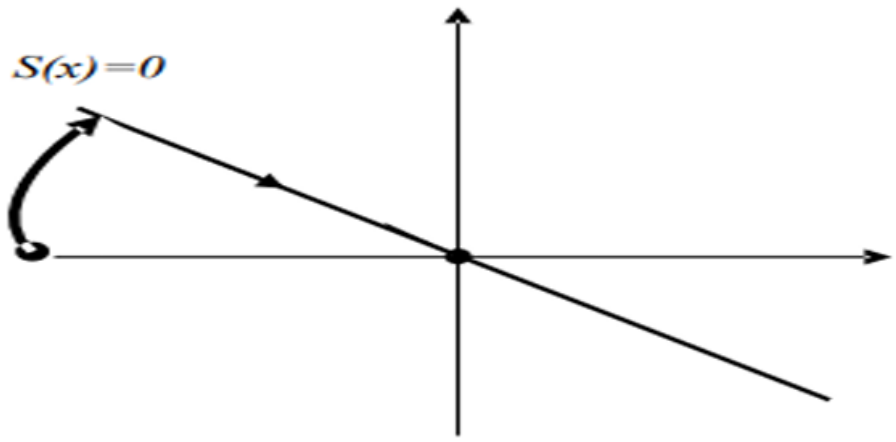

Figure III.2: Ideal Sliding Regime

In practice, the switching element consists of relays with inherent imperfections, such as switching delaysandhysteresis approximations. Additionally, the controller model itself relies on approximations. Consequently, the system's phase trajectory in the sliding regime remains close to the switchingsurfacebut does not follow it exactly. This results in undesirable oscillationsaround the sliding surface, commonly known **as** chattering**.**

While chattering does not typically compromise overall system stability, it reduces control accuracyand can lead toincreased wear and energy losses. ForSynchronousReluctanceMotors (SynRM)**,** such oscillations may generate mechanical vibrations and degrade performance. Therefore, minimizing chattering is a key objective in the design of robust sliding mode controllers.

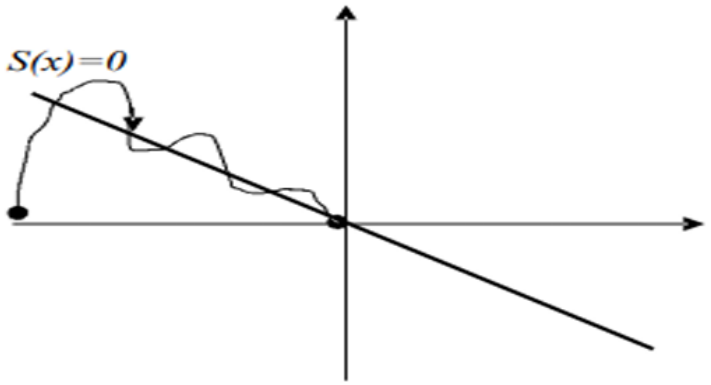

Figure III.3: Real Sliding Regime

III.2.4 Sliding Mode Control Design

The design of sliding mode controllers systematically addresses both stability issues **and** performance requirements of the controlled system. The design process is typically divided into three main steps:

- Selection of the sliding surfaces**:** Defining appropriate surfaces in the state space that the system trajectories will be driven to and constrained upon.
- Establishment of existence and convergence conditions**:** Ensuring that the system trajectories will reach the sliding surfaces in finite time and remain on them, which guarantee system stability.

- Determination of the control law**:** Designing the switching control strategy that drives the system states to the sliding surface and maintains the sliding motion.

In the context **of** Synchronous Reluctance Motors (SynRM)**,** these steps are crucial to achieve robust and high-performance torque and speed control, even in the presence of parameter uncertainties and external disturbances.

III.2.4.1 Choice of the Sliding Surface

The selection of the sliding surface involves determining not only the number of surfaces require**d**but also their specific expressions based on the application and control objectives**.**

The system can generally be represented as:

$$[\dot{x}]=[A].[x]+[B].[u] \quad \text{(III.1)}$$

Typically, the number of sliding surfaces corresponds to the dimension of the control input vectoru(t).The sliding surface S(x,t) is defined as:

$$S(x,t) = \left(\frac{\partial}{\partial t} + \lambda x\right)^{r-1} e(t) \quad \text{(III.2)}$$

where

- $e(t) = x_{ref}(t) - x(t)$ is the tracking error,
- λ is a positive constant that determines the desired control bandwidth,
- $\tau$is the relative degree, i.e., the number of times the output must be differentiated until the control input explicitly appears.

The sliding surface expression depends on the relative degreeτ:

- For $\tau = 1$ $\quad S(x) = e(x)$
- For $\tau = 2$ $\quad S(x) = \lambda \dot{e}(x) + e(x)$
- For $\tau = 3$ $\quad S(x) = \lambda^{2}\ddot{e}(x) + 2\lambda \dot{e}(x) + e(x)$

The control objective is to maintain the sliding surface at zero. This surface equation is a linear differential equation whose unique solution is e(x)=0, ensuring perfect tracking of the reference.

III.2.4.2 Existence and Convergence Conditions

To ensure that the system dynamics convergetowards the sliding surfaces, certain mathematical conditions must be satisfied. The literature highlights two main convergence criteria, both associated with the converging phase of the system state**:**

•**a.**Switching Function Condition (Emelyanov and Utkin Criterion)

This approach, developed by Emelyanov and Utkin**,** enforces a converging dynamic toward the sliding surface by directly shaping its evolution.

The condition is defined as:

$$S\dot{}(x)* S(x)<0 \quad \text{(III.3)}$$

This inequality ensures that the time derivative of the sliding surface leads the system **toward zero**, implying convergence to the surface [39].

•b.Lyapunov Function Method

A Lyapunov function is a scalar function V(x)>0.used to verify the stabilit**y** of nonlinear systems. It provides a measure of system energy that must decrease over time for stability to be guaranteed [39][38].

The typical Lyapunov function used in sliding mode control is:

$$V(x)=\frac{1}{2}S^2(x) \quad \text{(III.4)}$$

Its time derivative must satisfy:

$$\dot{V}(x)=S(x)\dot{S}(x) \quad \text{(III.5)}$$

This condition confirms that the system's state will **converge toward and remain on** the sliding surface$S(x) = 0$ (III.6)

III.2.4.3 Determination of the Control Law

Once the sliding surface and the convergence condition are defined, the next step is to formulate the control law that drives the controlled variable toward the surface and ensures its convergence to the equilibrium point, while maintaining the sliding mode existence condition.

The control input vector u (t) is generally composed of two parts:

$$U(t) = U_{eq}(t)+U_n(t) \quad \text{(III.7)}$$

$U_{eq}(t)$:Theequivalent control**,** a continuous signal that compensates the nominal system dynamics. It was introduced by FilippovandUtkinand is responsible for maintaining motion on the sliding surface**.**

U_n (t): The discontinuous **(switching) control** term, introduced to satisfy the **convergence condition** (from Equation III.7). This term plays a **crucial role** in the Sliding Mode Control (SMC) technique as it ensures robustness against external disturbances and model uncertainties.

a. Switching Function Form

The most common form of the discontinuous control law is given by:

$$U_n = K \cdot Sign(S(x)) \quad \text{(III.8)}$$

Where:

- K is a positive control gain that must be carefully chosen based on the magnitude of uncertainties and disturbances[37].
- Sign(S(x)) is the signum function**,** which introduces a discontinuous action to drive the system trajectory toward and maintain it on the sliding surface S(x)=0.

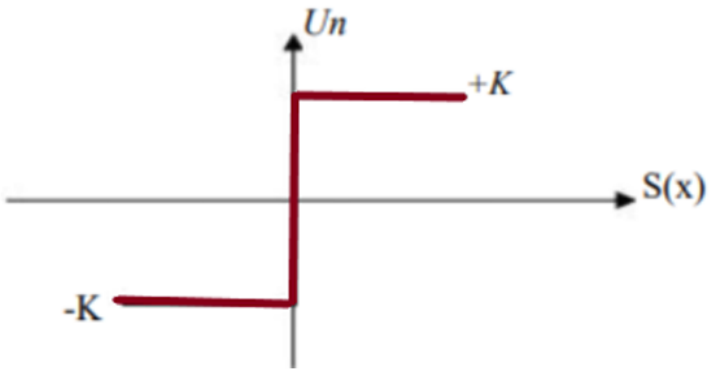

Figure III.4 – Sign Function Behavior

III.2.5 Sliding Mode Control of SynRM

We use first-order Sliding Mode Control (SMC) to create a reliable controller for the Synchronous Reluctance Motor (SynRM). This approach ensures accurate control over the motor's current and speed while effectively managing model uncertainties and external disturbances.

III.2.5.1Inside the d-q Reference Frame the SynRM Dynamic Model

The following equations represent the mathematical model of the SynRM in the spinning d-q frame:

$$\frac{di_d}{dt} = -\frac{R_s}{L_d} i_d + \omega_e \frac{L_q}{L_d} + \frac{1}{L_d} v_d \quad \text{(III.9)}$$

$$\frac{di_q}{dt} = -\frac{R_s}{L_q} i_q + \omega_e \frac{L_d}{L_q} + \frac{1}{L_q} v_q \quad \text{(III.10)}$$

$$\frac{d\Omega}{dt} = \frac{p}{J}\left(L_q - L_d\right) i_d i_q - \frac{f}{j}\Omega - \frac{1}{J} C_r \quad \text{(III.11)}$$

III.2.5.2 Definition of Sliding Surfaces

To implement the sliding mode control, we define the tracking error surfaces as:

$$S_\Omega(t) = \Omega_{ref}(t) - \Omega(t) \quad \text{(III.12)}$$

$$S_{\mathrm{iq}}(t) = \mathrm{iq}_{ref}(t) - \mathrm{i_q}(t) \quad \text{(III.13)}$$

$$S_{\mathrm{id}}(t) = \mathrm{id}_{ref}(t) - \mathrm{i_d}(t) \quad \text{(III.14)}$$

The goal is to regulate the rotor speed Ω, the torque-producing q-axis current iqi q, and the d-axis current idid, which is normally set to zero for maximum torque output and loss reduction. Robust trajectory tracking will be achieved by using these sliding surfaces to develop the control laws that guarantee the errors converge to zero in finite time.

III.2.6 Benefits and drawbacks of the command via sliding mode

III.2.6.1Broutementproblem

An ideal sliding regime requires a command that may be triggered periodically. Endless.Therefore, the discontinuity applied to the command peut during the sliding regime causes a phenomenon of shouting, known as "chattering" in English or "reticence." Broutement-related issues can reduce the mechanical system's performance by causing vibrations, consuming excessive amounts of energy, and shortening the lifespan of mechanical equipment (actionneurs). This is characterized by strong oscillations in the system's trajectory around the sliding surface (Fig.III.5). Because these lasts are not taken into consideration in the system modeling, this command results in increased high frequency dynamics, which may also cause the system to become unstable. [37] [39]

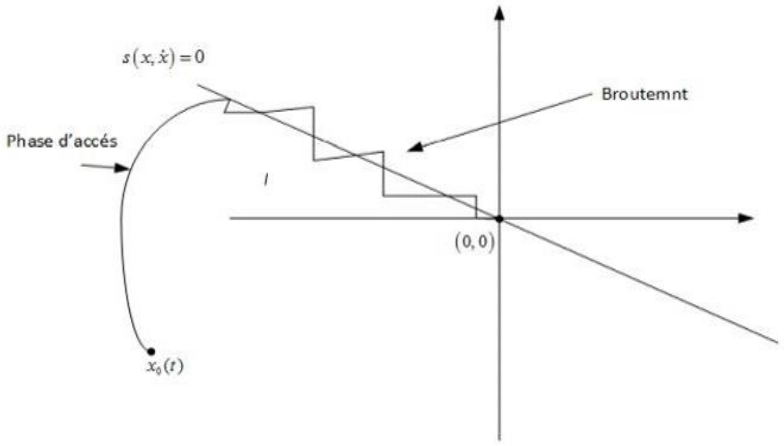

Figure III. 5: Chattering phenomenon

III.2.6.2 Reduction of the Chattering Phenomenon

A number of methods have been put forth to lessen or completely eradicate the chattering problem, which is a recognized disadvantage of traditional Sliding Mode Control (SMC). These consist of, among other things, fuzzy sliding mode control, higher-order sliding modes, the boundary layer approach, and approximated switching laws.

- **Solution by a Higher-Order Sliding Mode**

  The chattering issue has been tackled by introducing higher-order sliding mode control, which preserves the advantages of classical sliding mode control, including robustness against disturbances and model uncertainties and finite-time convergence.
  To enhance system performance, we use the second-order sliding mode technique in this work. In particular, we use the well-known methods listed below:

  -Algorithm with Super-Twisting
  -Algorithm Twisting

By removing the discontinuity in the control signal's first derivative, these methods produce smoother control actions and less chattering. They work especially well with systems like the SynRM, where high-frequency switching can create noise and unintended mechanical stress.

III.3 Second Order Sliding Mode control

III.3.1 Principle

In the 1980s, M. Emelyanov and M. Levantovsky established the idea of Higher-Order Sliding Mode Control (HOSMC). HOSMC approaches work on the higher derivatives of the sliding variable, which improves performance and lowers control discontinuities compared to traditional first-order sliding modes.

The chattering problem, which arises from high-frequency switching and can have unintended consequences, particularly in electromechanical systems like Synchronous Reluctance Motors (SynRM), is one of the primary drawbacks of traditional Sliding Mode Control (SMC). This sophisticated control approach tackles this issue.

In this study, we concentrate on the second-order sliding mode control (SOSMC) method, which works especially well for systems with relative degree two and where maintaining actuator and motor integrity requires minimizing chattering.

The main benefit of using this sliding mode for command is that it can identify chattering phenomena. Its goal is to create a two-order sliding regime on the chosen glide surface S = 0 and obtain the final time S = $\dot{S}$ = 0.

$$\ddot{x} = (x,t) + g(x,t) * u \tag{III.15}$$

The goal is to create a sliding regime of order two relative to S by forcing the system's state trajectory to change over a finite amount of time on the whole S_2 ensemble and then stopping it afterwards:

$$S_2 = \{x : s = \dot{s} = 0\} \tag{III.16}$$

This is accomplished via command acting on the second derivative of the glissement variable, which may be expressed generally as follows:

$$\ddot{s} = (x,t) + \phi(x,t).v \tag{III.17}$$

With:

$v = \dot{u}$ Case of Relative Degree n=1with Respect to Si .e$\frac{\partial}{\partial u}\dot{s} \neq 0$

$v = u$in the case where the system has a relative degree n=2 with respect to s, i.e. $\frac{\partial}{\partial u}\ddot{s} \neq 0$

To implement second-order sliding mode algorithms, it is necessary to verify the following working hypothesis in order to validate the reachability of the sliding surface and the boundedness of the variable S:

- The uncertain functions ϕ(x,t)and φ(x,t) are bounded.
- There exist four positive constants S0,C0,Km,KM such that, in a neighborhood where |S(x,t)|<S0 , the following inequalities hold:

$$|\varphi(x,t)| < C0 \ and \ 0 < Km \leq \phi(x,t) \leq KM \tag{III.18}$$

The above assumptions imply that the second derivative of the switching function is uniformly bounded in a certain domain $\varepsilon_l$for the considered input.

By satisfying the previously defined conditions, we can write that any solution related to equation (III.17) satisfies the following differential inclusion:

$$\dot{S} \in [-C0, C0] + [Km, KM] \cdot v \qquad \text{(III.19)}$$

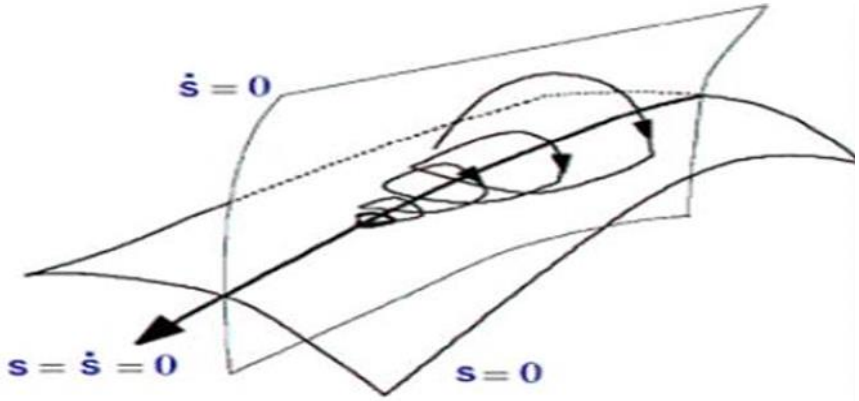

Figure III.6: Trajectory of the Second-Order Sliding Mode

III.3.2 Examples of Second-Order Sliding Mode Control Algorithms

Several second-order sliding mode control (SOSMC) algorithms have been proposed by researchers. Amongthem are:

- Twisting Algorithm
- Super-Twisting Algorithm
- Sub-Optimal Algorithm
- Drift Algorithm

III.3.3 Super Twisting Algorithm

By managing systems with a relative degree of one, the Super Twisting algorithm was developed to stop chattering.This control law was first presented by Emelyanov in 1990 [37].The converge nce of this algorithm is likewise controlled by rotations around the origin of the phase diagram.T he Super Twisting control law U(t) is obtained by combining two terms (see Eq. III.20).The first term is defined by its time derivative (Eq. III.21), whereas the second term is given by a continuo us function of the sliding variable (Eq. III.22) [38]

The following is the control law:

$$u = k_P.|s|^{1/2}.sign(s) + \int k_I.sign(s) \quad \text{(III.20)}$$

Where:

- *s* is the sliding surface.
- *u* is the control input.
- K_P, K_I are positive control gains.

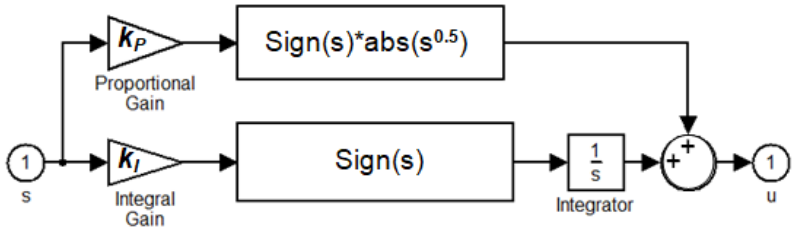

Figure III.7: Block diagram of STC

This algorithm's strength lies in the fact that it doesn't require knowledge of the S derivation. Because of this feature, it is possible to decrease the system's capteur counts and calculation times [37].

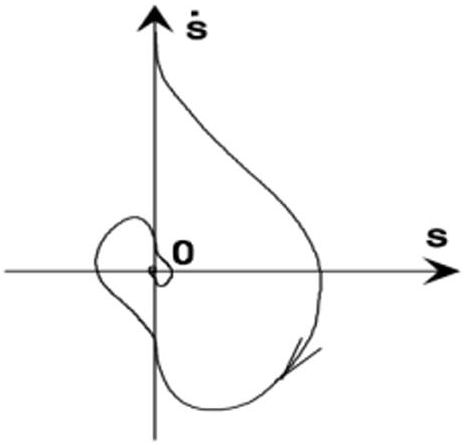

Figure III. 8: Super-Twisting algorithm convergence in the plan ($S\dot{S}$)

The algorithm's trajectory in the phase plan($S\dot{S}$) is shown in figure (III.6), where it is demonstrated that the successive crossings of that ci with the plan's axes evolve while reproaching the initial value, which is reached at the end of time. [40]

III.4. Proposed PID-Gain-Based Super-Twisting Controller (PID-STC)

III.4.1. PID-STC Controller design

In order to improve the performance of the classical Super-Twisting Algorithm (STA), a modified version is proposed that incorporates a derivative term of the sliding surface into the control law. This enhancement is motivated by the analogy between the STA and a nonlinear PI controller. Just as PID controllers extend PI action by adding a derivative component to improve dynamic response and reduce overshoot, this approach introduces a derivative-based nonlinear gain to the STA to form a PID-like Super-Twisting Controller (PID-STC).

The resulting control law integrates three terms with nonlinear gains: proportional, integral (standard in STA), and derivative actions with respect to the sliding variable. This structure not only improves tracking precision during the sliding phase but also further attenuates chattering, which is a common drawback in discontinuous sliding mode controllers.

The control input is defined as follows:

$$u = k_P.|s|^{1/2}.sign(s) + \int k_I.sign(s) + \frac{d}{dt}\left(k_D.sign(s)\right) \qquad \text{(III.21)}$$

The proposed controller law is composed of three terms as below:

- The proportional term is |s|1/2·sign(s),
- The integral action is of the form ∫sign(s), as in classical STA,
- The derivative action is $\frac{d}{dt}(k_D.sign(s))$

Where:

- s is the sliding surface,
- u is the control signal,
- k_P,k_I,k_D are strictly positive nonlinear gains associated with the proportional, integral, and derivative actions, respectively.

This improved controller, denoted PID-STC, preserves the finite-time convergence property of the classical STA while offering enhanced robustness and reduced chattering in the presence of disturbances or model uncertainties.

The block diagram illustrating the proposed PID-STC is shown in figure III.9.

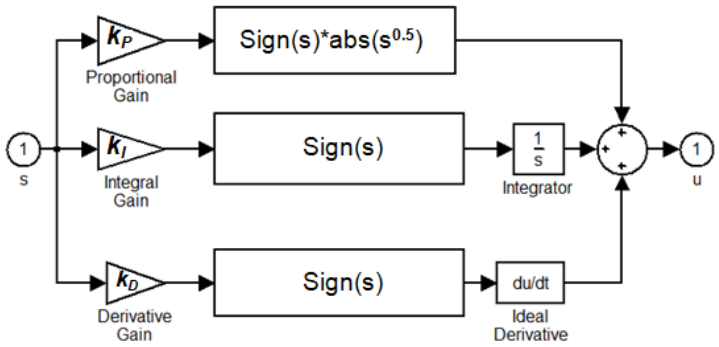

Figure III.9: Block diagram illustrating the proposed PID-STC

III.4.2. Stability Study of the Proposed PID-STC using Lyapunov theory

To study the stability of the proposed PID-like Super-Twisting Controller with a derivative of sign(s) using Lyapunov theory, we proceed step by step.

We consider the control law given by the equation (III.22). We consider a general first-order system:

$$\dot{s} = f(t) + g(t)u + d(t) \tag{III.22}$$

where:

- $g(t) \geq g_{min} > 0$,
- $d(t)$ is a matched bounded disturbance, i.e., $|d(t)| \leq d_{max}$.

Substitute u into $\dot{s}$:

$$\dot{s} = f(t) + g(t)\left[.|s|^{\frac{1}{2}}.sign(s) + \int k_I.sign(s) + \frac{d}{dt}\left(k_D.sign(s)\right)\right] + d(t) \tag{III.23}$$

We define the states variables:

- $\eta(t) = \int sign(s)dt$
- $\sigma(t) = sign(s)$
- $\xi(t) = \frac{d}{dt}\left(k_D.sign(s)\right)$

The control law becomes:

$$u = k_P.|s|^{1/2}.sign(s) + \eta(t) + k_D.\xi(t) \quad \text{(III.24)}$$

We propose the following Lyapunov function involving all three states:

$$V = \frac{1}{2}s^2 + \frac{1}{2}\eta^2 + \frac{1}{2}\xi^2 \quad \text{(III.25)}$$

V>0 for all $(s,\eta,\xi) \neq 0$ and $V=0$ only at the origin.

Differentiate:

$$\dot{V} = \dot{s}s + \dot{\eta}\eta + k_D.\dot{\xi}\,\xi \quad \text{(III.26)}$$

We know:

- $\dot{\eta} = sign(s)$
- $\xi = \dot{\sigma}$,and in distribution sense:

$$\dot{\sigma} = 2\delta(s)\,.\dot{s} \quad \text{(III.27)}$$

In practical implementation$\dot{\sigma} \approx \frac{d}{dt}(\tanh(\frac{s}{\phi}))$

Now:

$$\dot{V} = s\dot{s} + \eta.sign(s) + K_D\xi\dot{\xi} \quad \text{(III.28)}$$

Substitute :

$$\dot{s} = -g(t)\left(k_p|s|^{\frac{1}{2}}.\sigma + k_I\eta + K_D\xi\right) + d(t) \quad \text{(III.29)}$$

Then:

$$\dot{V} = \left[-g(t)\left(k_p|s|^{\frac{1}{2}}.\sigma + k_I\eta + K_D\xi\right)\right] + \eta\sigma + K_D\xi\dot{\xi} \quad \text{(III.30)}$$

Let's analyse term-by-term under the assumption that $sign(s) = \sigma$, and the signals are smoothed:

- $s.\sigma = |s|$
- $s.|s|^{\frac{1}{2}}.\sigma = |s|^{3/2}$
- $s\eta = sign(s).|s|.\eta$
- $\eta\sigma = |\eta|$
- Assume $\xi\dot{\xi} \leq 0$(stabilizing due to sign derivative)

Using bounds $g(t) \geq gmin$, we write:

$$\dot{V} \leq g_{min} k_p |s|^{\frac{3}{2}} - g_{min} k_{Is\eta} - g_{min} k_{DS\xi} + |s| d_{max} + |\eta| + K_D \xi \dot{\xi} \quad \text{(III.31)}$$

Assuming that:

- $s\eta > 0$
- $s\xi > 0$

$\xi\xi \dot{\leq} 0$ (as in bounded sliding dynamics)

Then all first three terms are negative, and only disturbances remain.

We conclude that:

- The Lyapunov function *V(s,η,ξ)* is positive definite,
- Its derivative $\dot{V}$ *i*s negative definite outside a small neighbourhood**,**
- Hence, the closed-loop system is uniformly ultimately bounded (UUB)**,**
- In the absence of disturbances, the system converges asymptotically (and potentially in finite time under stronger conditions).

The proposed PID-STC controller ensures the stability of the closed-loop system. Using a Lyapunov function that includes the state *s*, its integral *η*, and the derivative *ξ*, we demonstrate that the system is uniformly ultimately bounded (UUB**)** in the presence of matched disturbances, and asymptotically stable in the ideal case. The derivative term improves responsiveness and robustness by introducing higher-order sliding behavior.

III.5 Using PID-STC to control the SynRM

The PID-STC is a robust command-by-second-order sliding strategy that is especially useful for increasing robustness against uncertainties and lowering chattering. This algorithm is applied to three fundamental grandeurs inside the framework of a FOC of a SynRM; the rotational velocity Ω, the direct current I_d, and the quadratic current I_q.

III.5.1. Control of the rotational speed Ω:

The discrepancy between the measured and reference speeds is

$$e_\Omega = \Omega - \Omega^* \quad \text{(III.32)}$$

The sliding surface is

$$S_1 = e \quad \text{(III.33)}$$

The super-twisting command that is applied is

$$T_{em}^{*} = k_{P\Omega}.|S_1|^{1/2}.sign(S_1) + k_{I\Omega}\int sign(S_1)dt + K_{D\Omega}\frac{d}{dt}\big(sign(S_1)\big) \quad \text{(III.34)}$$

III.5.2. Control of the direct statoric current I_d:

The definition of a regulation error is as:

$$e_d = I_d - I_d^{*} \quad \text{(III.35)}$$

An associated sliding surface is defined:

$$S_2 = e_d \quad \text{(III.36)}$$

The extremely twisted command entry for I_d is then:

$$v_d = k_{Pd}.|S_2|^{1/2} + k_{Id}\int sign(S_2)dt + K_{D\Omega}\frac{d}{dt}(sign(S_2)) \quad \text{(III.37)}$$

III.5.3. Control of the quadratic statoric current I_q:

The error is provided by

$$e_q = I_q - I_q^{*} \quad \text{(III.38)}$$

The corresponding sliding surface

$$S_3 = e_q \quad \text{(III.39)}$$

Super-twisting command to adjust the currentIq (the couple's responsibility)

$$v_q = k_{Pq}.|S_3|^{1/2} + k_{Iq}\int sign(S_3)dt + K_{Dq}\frac{d}{dt}(sign(S_3)) \quad \text{(III.40)}$$

III.6 Simulation results of PID-STC Applied to the SynRM

III.6.1 References tracking test:

The effectiveness of the proposed PID-STC control strategy for speed regulation of the Synchronous Reluctance Motor (SynRM) has been validated through comprehensive numerical simulations. The test scenario included a step change in speed reference of 100 rad/s, along with a reversal in the direction of rotation at t=2.5. Furthermore, a load disturbance of 15 N·m was introduced between t=1 s and t=4 to evaluate the robustness of the controller.

Figures III.10 to III.11 present the simulation results obtained with the PID-STC regulator, which also includes stator current limitation to enhance hardware protection. The main findings are summarized below:

- *Rotor Speed Tracking (Ω):* The rotor speed exhibits excellent reference tracking performance across all phases of operation, including during the application of the 15 N·m load disturbance. A minimal transient deviation is observed upon disturbance application; however, the system promptly compensates for this, showcasing the superior disturbance rejection capabilities of the PID-STC.
- *Electromagnetic Torque Response (Tem):* The torque response demonstrates a rapid rise during startup, followed by smooth convergence to the steady-state torque level. This confirms the controller's capacity for precise and fast torque regulation.
- *Direct-Axis Current (Id):* The direct-axis current remains effectively close to zero under all operating conditions, which validates the efficacy of the decoupling mechanism in the implemented vector control structure.
- *Quadrature-Axis Current (Iq):* The quadrature-axis current closely matches the torque demand, confirming that the electromagnetic torque is accurately controlled via this component, as expected in field-oriented control strategies.
- *Stator Phase Currents:* The phase currents exhibit clean sinusoidal waveforms with low harmonic content, reflecting proper inverter operation and confirming that the vector control strategy ensures balanced and high-quality current profiles.

Although the system demonstrates remarkable performance overall, transient overcurrents in Id and Iq are noted during dynamic phases such as startup and disturbance application. These overcurrents, while temporary, may stress the inverter components. To mitigate this, stator current limitation has been integrated into the PID-STC algorithm, effectively bounding these peaks without degrading control performance.

Under the proposed PID-STC scheme, the SynRM drive exhibits excellent dynamic behavior, characterized by fast convergence, strong disturbance rejection, and high-quality current waveforms. The enhanced performance in both steady-state and transient conditions confirms the robustness and efficacy of the PID-STC, making it a viable solution for high-performance SynRM applications.

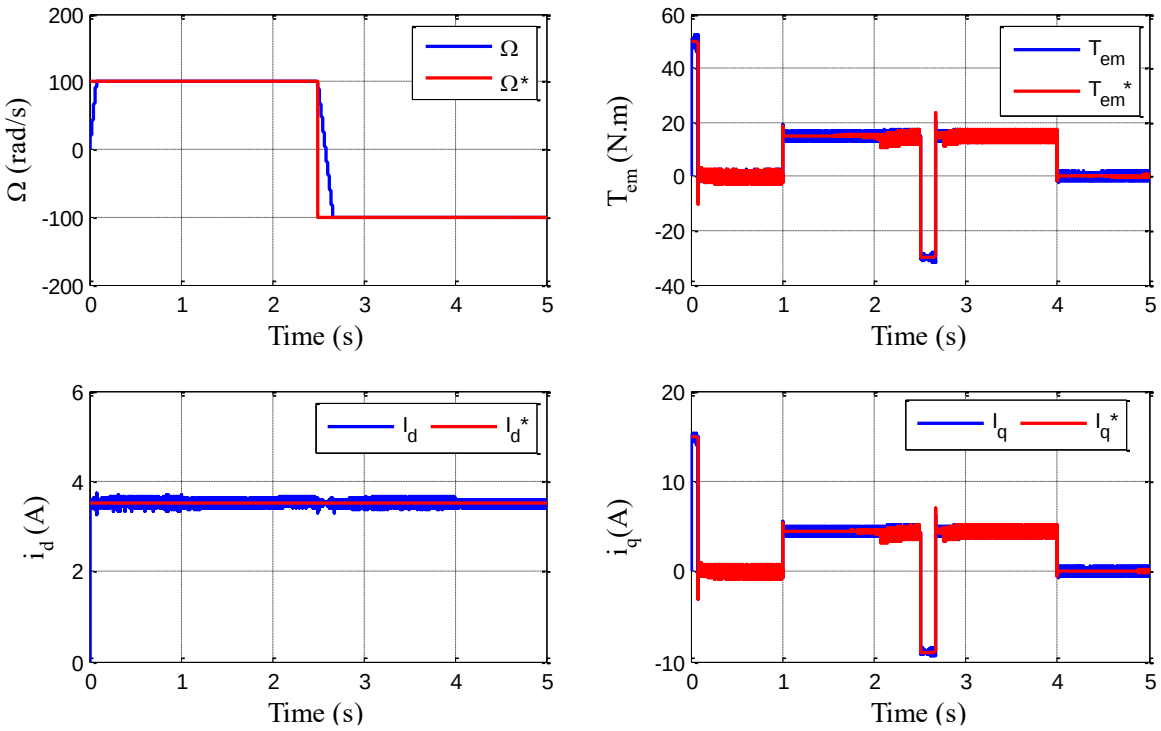

Figure III.10: Speed regulation (with PI controller) of the SynRM using vector control for a reference speed of $\pm 100\,rd/s$, with load disturbance of 15 N·m was applied between t = 1 s and t = 4 s.

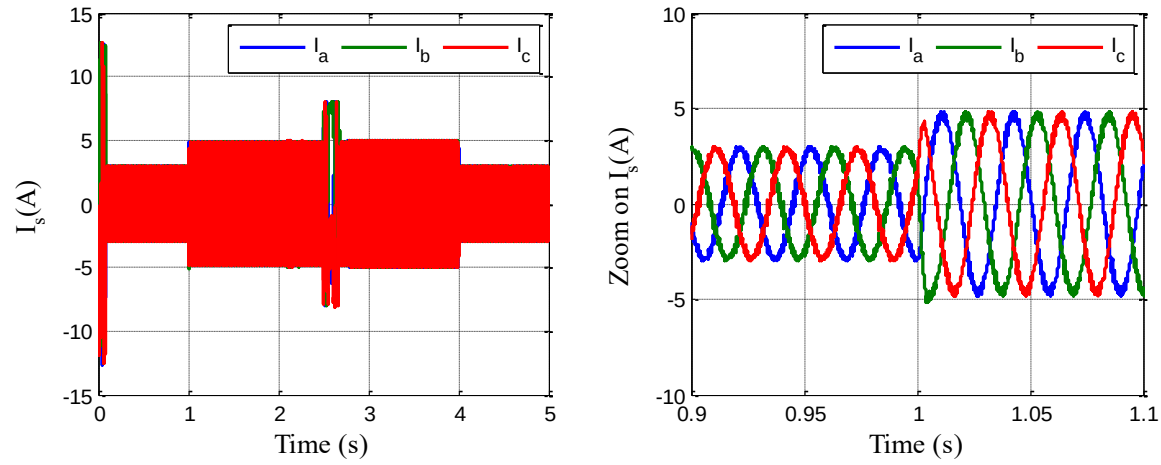

Figure III.11:Three Phase Stator Currents of the SynRM using vector control for a reference speed of $\pm 100\,rd/s$, with load disturbance of 15 N·m was applied between t = 1 s and t = 4 s.

II.6.2. Robustness Test under parametric uncertainty

The robustness of the proposed PID-STC controller is evaluated under extreme parameter mismatches. During the simulation, the SynRM is operated under indirect vector control with rotor flux orientation. While the control algorithm uses nominal machine parameters**, the** actual machine model is subjected to deliberate variations, introduced at a specific simulation time. These variations are as follows (see Figure III.12):

- **A** +100% increase in stator resistanceR_s**,**
- **A** −100% reduction in both direct- and quadrature-axis inductances$L_d$andL_q**,**
- **A** +100% increase in moment of inertia$J$**.**

For the speed response *(Ω)*, The PID-STC controller demonstrates excellent robustness in speed regulation, despite the substantial parameter deviations. The rotor speed closely tracks the reference profile without any significant overshoot or delay, even during critical dynamic phases such as startup and reversal. Unlike conventional PI-based control, which typically suffers from increased response time and overshoot, the PID-STC maintains fast convergence and accurate steady-state tracking. This clearly highlights the controller's low sensitivity to model uncertainties and its strong disturbance rejection capability. For the Electromagnetic Torque (Tem), theresponse remains well-aligned with the reference, both in transient and steady-state conditions. Even with altered inductance and increased inertia, the PID-STC ensures precise torque control without the degradations typically observed in PI-regulated systems. The chattering-free nature of the super-twisting structure, combined with the derivative correction, provides enhanced torque dynamics and resilience to parameter mismatches**.**

About the flux Components (Id and Iq): The stator flux components maintain their decoupling structure throughout the simulation. The direct-axis current IdI_dId remains near zero, confirming accurate field orientation, while the quadrature-axis current IqI_qIq continues to reflect the torque demand appropriately. The control law ensures that flux regulation is minimally impacted by inductance variations, demonstrating the internal robustness of the PID-STC under rotor-oriented control.

The stator phase currents maintain balanced and nearly sinusoidal waveforms, ensuring good power quality. Although a slight increase in current amplitude is noted—primarily due to the doubled stator resistance—the PID-STC effectively limits overcurrents through its embedded current limitation strategy. As a result, the thermal stress on the inverter and machine remains controlled, which is crucial for ensuring long-term system reliability under uncertain conditions.

The simulation results confirm that the proposed PID-STC controller offers superior robustness compared to traditional PI approaches, particularly in the presence of severe parameter

mismatches. The controller guarantees stable speed and torque regulation, accurate flux orientation, and high-quality current waveforms. These features make the PID-STC an excellent candidate for high-performance SynRM drives operating under uncertain or time-varying machine parameters.

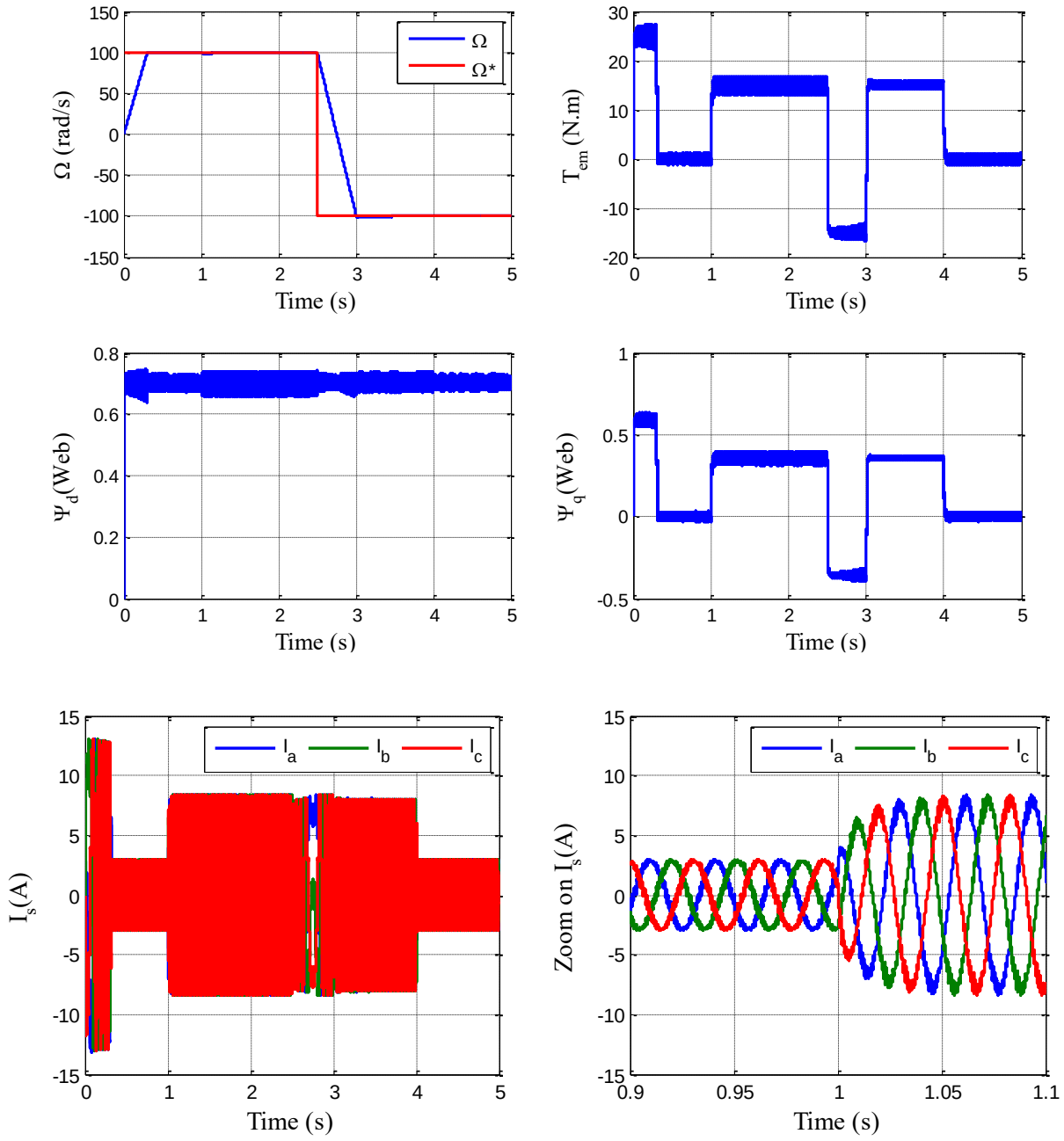

Figure III.12: Test de robustesse pour le réglage de vitesse de la SynRM (sous une charge nominale) par la commande vectorielle

III.7 Comparative Analysis of performance between PI, STC and PID-STC controllers

A comprehensive comparison was conducted between three control strategies applied to the speed regulation of the Synchronous Reluctance Motor (SynRM): the conventional Proportional-Integral (PI) controller, the classical Super-Twisting Controller (STC), and the proposed PID-STC controller, which incorporates an explicit derivative action. The focus of this analysis was on the controllers' ability to accurately track reference signals, particularly under variations in setpoint and system disturbances.

The simulation results, shown in Figures III.13 and III.14, clearly highlighted the limitations of the PI controller, especially in terms of response time, overshoot, and sensitivity to parameter variations. Although the classical STC demonstrated improved robustness against uncertainties and external disturbances, it exhibited a slower transient response and a noticeable chattering effect.

In contrast, the proposed PID-STC controller successfully combined the advantages of both previous approaches. The inclusion of an explicit derivative term within the Super-Twisting framework significantly enhanced transient performance while preserving robustness. The PID-STC exhibited superior performance in terms of fast convergence, precise setpoint tracking, minimal overshoot, and almost complete elimination of chattering.

These findings validate the effectiveness of the proposed PID-STC strategy in controlling systems under variable or uncertain operating conditions. Moreover, they highlight its clear superiority over classical controllers for robust control of electric machines.

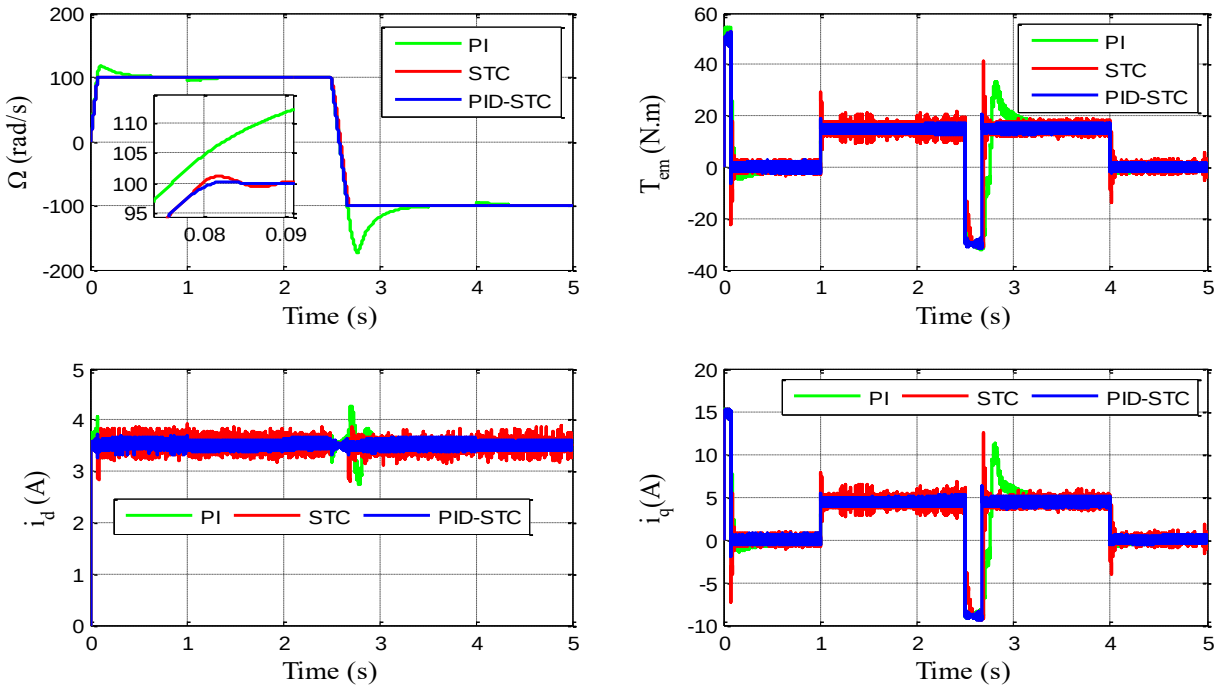

Figure III.13: Comparative Performance Analysis of the Controllers (PI, STC, PID-STC) in Terms of Reference Tracking Capability

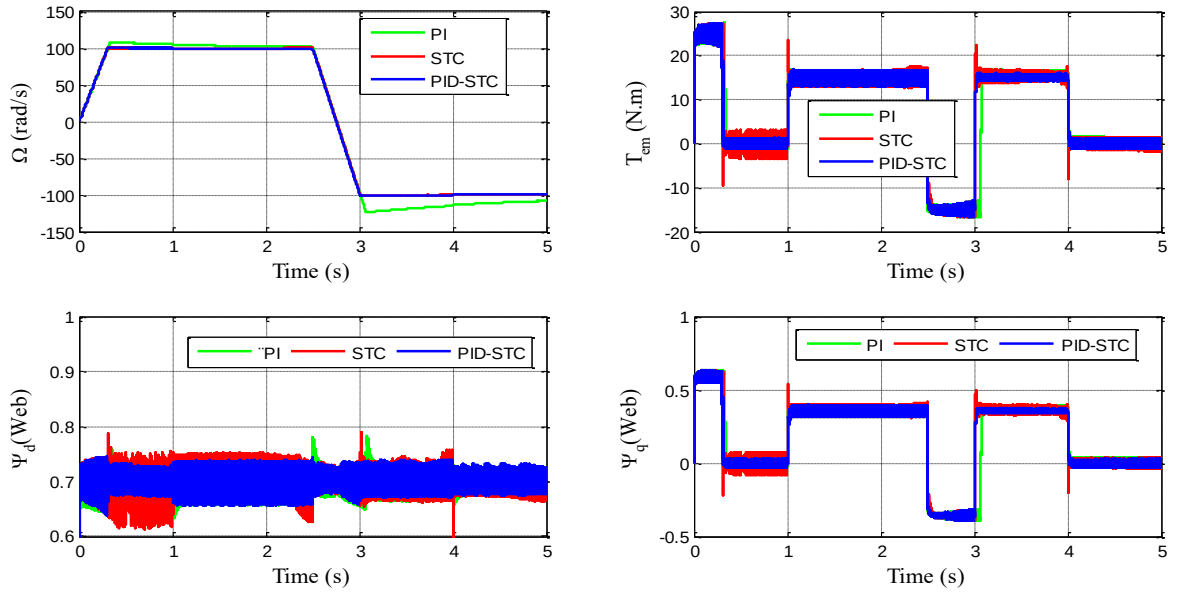

Figure III.14: Comparative Performance Analysis of the Controllers (PI, STC, PID-STC) in Terms of Robustness Capability to parameter variations

III.8 Conclusion

In this chapter, a robust and enhanced control strategy based on the Super-Twisting Algorithm (STA) augmented with PID-like gains has been successfully developed and applied to the speed regulation of a Synchronous Reluctance Motor (SynRM). The proposed PID-STC controller integrates proportional, integral, and discontinuous derivative actions into the sliding mode framework, offering improved transient performance, chattering attenuation, and robustness against model uncertainties and external disturbances.

Comprehensive simulation results have demonstrated the effectiveness of the controller in achieving fast dynamic response, precise reference tracking, and strong insensitivity to variations in motor parameters such as stator resistance and inductance. Compared to conventional PI and classical STC controllers, the proposed PID-STC exhibits superior control performance in terms of reduced overshoot, faster settling time, and minimized steady-state error.

Overall, this approach represents a promising solution for high-performance, model-insensitive control of SynRM drives, particularly in applications requiring reliability under variable operating conditions. Future work may extend this method to multi-variable systems or explore its real-time implementation on embedded hardware platforms.

General Conclusion

This final project has addressed the modeling and advanced control of Synchronous Reluctance Motors (SynRMs), with a focus on achieving high performance, robustness, and reliable operation under varying conditions.

The work began with a thorough investigation of the physical and mathematical foundations of SynRM operation. The machine's torque generation mechanism—rooted in magnetic reluctance—was analyzed, and its mathematical model in the d-q rotating reference frame was established. This initial study revealed the intrinsic nonlinear coupling between flux and torque, highlighting the complexity of controlling SynRMs and the necessity for decoupling strategies.

In the second part of the thesis, a vector control approach based on stator flux orientation was implemented to decouple flux and torque components. Under nominal conditions, this method demonstrated satisfactory dynamic behavior and control accuracy. However, simulations under parameter variations such as increased resistance and reduced inductance revealed performance limitations, including degraded torque tracking and increased thermal stress. These findings underlined the need for more robust control methods, particularly under non-ideal operating conditions.

To overcome these challenges, the third part of the work proposed a novel control scheme based on the Super-Twisting Sliding Mode Control (STC) algorithm enhanced with PID gains. This PID-STC controller effectively combines robustness, chattering reduction, and improved transient response. Through extensive simulation studies, the proposed approach showed superior performance over conventional PI and classical STC controllers, with faster dynamic response, better tracking accuracy, and strong robustness to parameter uncertainties.

In conclusion, this final year project has demonstrated that the proposed PID-based Super-Twisting control strategy is a powerful solution for the robust and precise control of SynRM drives. It effectively addresses the inherent nonlinearities and parameter dependencies of SynRMs, making it suitable for demanding applications where reliability and performance are critical. Future work may explore real-time hardware implementation, extension to multi-variable systems, or adaptation to other types of electrical machines requiring high robustness and dynamic precision.

Annexe

A1. The machine parameters used in the simulation:

Parameter	Value	Unit
Frequency	50	Hz
Stator resistance	7.8	
Pole pairs	2	
Inductance(*d-axis)*	0.4	H
Inductance(*q-axis)*	0.08	H
Inertia	0.038	$Kg.m^2$

A2. Regulators parameters used in the simulation

Parameter
$K_{i\Omega} = (W_n * J)$
$K_{p\Omega} = (2 * W_n * J)$
$K_i I_d = L_d * (W_n \wedge 2)$
$K_p I_d = (2 * W_n * L_d) - R_s$
$K_i I_q = L_q * (W_n \wedge 2)$
$K_p I_p = \left(2 * W_n * L_q\right) - R_s$
$W_n = 314$
$\mathrm{I}_{\mathrm{dref=3.5}}$

$$A_1 = \begin{bmatrix} -\frac{R_s}{L_d} & 0 \\ 0 & -\frac{R_s}{L_q} \end{bmatrix}$$

$$A_2 = \begin{bmatrix} 0 & \frac{L_q}{L_d} \\ -\frac{L_d}{L_q} & 0 \end{bmatrix}$$

$$B_1 = \begin{bmatrix} \frac{1}{L_d} & 0 \\ 0 & \frac{1}{L_q} \end{bmatrix}$$

References

[1] Boldea, I. Electric Machines: Steady-State, Transients, and Design with MATLAB**.** CRC Press, 2021.

[2] Krishnan, R. Electric Motor Drives: Modeling, Analysis, and Control. Pearson Education, 2001.

[3] Vagati, A., Pastorelli, M., and Tenconi, A. "Impact of PM motor technology on industrial drives." *IEEE Transactions on Industrial Electronics*, 1998.

[4] Miller, T.J.E. Switched Reluctance Motors and Their Control. Oxford University Press, 1993.

[5] Pyrhönen, J., Jokinen, T., and Hrabovcova, V. Design of Rotating Electrical Machines, Wiley, 2008.

[6] El-Refaie, A.M. "Motors/generators for traction/propulsion applications: A review." *IEEE Transactions on Vehicular Technology*, 2010.

[7] Vas, P. Sensorless Vector and Direct Torque Control. Oxford University Press, 1998.

[8] Leonhard, W. Control of Electrical Drives. Springer, 2001.

[9] Utkin, V.I. "Sliding mode control design principles and applications to electric drives." *IEEE Transactions on Industrial Electronics*, 1993.

[10] Levant, A. "Sliding order and sliding accuracy in sliding mode control." *International Journal of Control*, 1993.

[11] Levant, A. "Higher-order sliding modes, differentiation and output-feedback control." *International Journal of Control*, 2003.

[12] Fridman, L., Moreno, J.A., and Iriarte, R. Sliding Mode Control: Theory and Applications. Springer, 2011.

[13] Anouar Boukhalouf, contribution à la commande des système non linéaires : application à la machine synchrone à réluctance variable.université Mohamed Khider-Biskra,2022/2023.

[14] Thierry Lubin. Modélisation et commande de la machine synchrone à réluctance variable: prise en compte de la saturation magnétique. PhD thesis, Université Henri Poincaré; Nancy I, 2003

[15] DAStaton, TJE Miller, and SE Wood. Maximising the saliency ratio of the synchronous reluctance motor. In IEE Proceedings B (Electric Power Applications), volume 140, pages 249–259. IET, 1993.

[16]PhuocHoa TRUONG. Optimisation des performances de la machine synchrone à réluctance variable: approches par la conception et par la commande. PhD thesis, Université de Haute-Alsace, 2016.

[17] SeyedMortezaTaghavi and PragasenPillay. A mechanically robust rotor with transverse laminations for a wide-speed-range synchronous reluctance traction motor. IEEE Transactions on Industry Applications, 51(6):4404– 4414, 2015.

[18] Synchronous reluctance machine, https : //pnbalamurugan.yolasite. com

[19] What is synchronous reluctance motor &its working, https:// www.elprocus.com.

[20]HARI PRASANTH SUNDARA MURTHY, “Synchronous Reluctance Motors and PM Assisted Synchronous Reluctance Motors: Rotor Configuration, Design Aspects, Performance Comparison, id10592833, 2020/2021.

[21]: epochautomation, special motors, synchronous reluctance motors-advantage and disadvantage, february3, 2023,https://epochautomation.com.

[22]BELKACEM Salma, optimisation énergétique d’un système éolien basé sur un générateur à reluctance synchrone (synrm)“energyoptimization of a wind system based on a synchronous reluctance generator (synrm) , Hassiba ben bouali

[23]. Heidari, H.; Rassõlkin, A.; Kallaste, A.; Vaimann, T.; Andriushchenko, E.; Belahcen, A.; Lukichev, D.V. A reviewofsynchronous reluctance motor-drive advancements. Sustainability 2021, 13, 729. [CrossRef]

[24]. Pellegrino, G.; Jahns, T.; Bianchi, N.; Soong, W.; Cupertino, F. The Rediscovery of Synchronous Reluctance and Ferrite Permanent Magnet Motors; Springer International Publishing: Berlin/Heidelberg, Germany, 2016.

[25]. Baimel, D.; Belikov, J.; Guerrero, J.M.; Levron, Y. Dynamic modeling of networks, microgrids, and renewable sources in the dq0 reference frame: A Survey. IEEE Access 2017, 5, 21323. [CrossRef]

[26]. Levron, Y.; Belikov, J.; Baimel, D. A tutorial on dynamics and control of power systems with distributed and renewable energy sources based on the dq0 transformation. Appl. Sci. 2018, 8, 1661. [CrossRef]

[27]. Sul, S.K. Control of Electric Machine Drive Systems; John Wiley and Sons: Hoboken, NJ, USA, 2011.

[34]. Betz, R.E.; Lagerquist, R.; Jovanovic, M.; Miller, T.J.E.; Middleton, R.H. Control of synchronous reluctance machines. IEEE Trans. Ind. Appl. 1993, 29, 1110–1122. [CrossRef]

[28]. Hadla, H. Predictive Load Angle and Stator Flux Control of SynRM Drives for the Full Speed Range. Ph.D. Dissertation, Coimbra University, Coimbra, Portugal, August 2018.

[29].Yamamoto, Shu, Takuya Kojima, and Hideaki Hirahara. "Mathematical Models of Synchronous ReluctanceMotor Considering Iron Loss and Cross-Magnetic Saturation with Reciprocity Relation of Mutual Inductance."IEEJ Journal of Industry Applications 11, 2022, no. 1, 206-215.

[30] Accetta, Angelo, Maurizio Cirrincione, Marcello Pucci, and AntoninoSferlazza. "Space-vector state dynamic model of the synchronous reluctance motor considering self, cross-saturation and iron losses." In 2021 IEEEEnergy Conversion Congress and Exposition (ECCE), 2021, pp. 4164-4170.

[33]. Li C, Wang G, Zhang G et al (2019) Saliency-based sensorless control for synrm drives with suppression of position estimation error. IEEE Trans Ind Electron 66:5839–5849. https://doi.org/10. 1109/tie.2018.2874585

[31]. D A Staton, T J E Miller, S E Wood. Maximising the saliency ratio of the synchronous reluctance motor. IEE Proceedings B (Electric Power Applications), 1993, 140(4): 249-259.

[32]. R E Betz, R Lagerquist, M Jovanovic, et al. Control of synchronous reluctance machines. Transactions on Industry Applications, 1993, 29(6): 1110-1122.

[33]. Li C, Wang G, Zhang G et al (2019) Saliency-based sensorless control for synrm drives with suppression of position estimation error. IEEE Trans Ind Electron 66:5839–5849. https://doi.org/10. 1109/tie.2018.2874585

[34]. Betz, R.E.; Lagerquist, R.; Jovanovic, M.; Miller, T.J.E.; Middleton, R.H. Control of synchronous reluctance machines. IEEE Trans. Ind. Appl. 1993, 29, 1110–1122. [CrossRef]

[35]. BOUDJEMA ABDE RAOUF, Commande vectorielle de la machine synchrone à aimants permanents MSAP, Mémoire de Master, Université de Biskra, 2014.

[36]. F. Benchabane, “Commande en position et en vitesse par mode de glissement d‟un moteur synchrone triphasé à aimants permanents avec minimisation du chattring”,Thèse de Magister, Université de Biskra, 2005.

[37]. C T Liu, P C Shih, S C Yen, et al. Theoretical and experimentalinvestigations of the electromagnetic steel compositions for synchronous reluctance motors. Transactions on Industry Applications, 2018, 54(3): 2947-2954.

[38] N. Rassouad and D. Touati, "Optimization of the command parameters by mode glissant of order 2 of the speed of an MSAP"Université Tlemcen, Master's Memoir, 2020–2021.[32] N. Bounasla, "Directed by the Guidance of the Supérieur Order of the Synchrone Mac hine to Permanent Aimants"Université Sétif, Mémoire de Magister, 2013/2014

[39] CH. Hadjaziet KH. Kerroumi "Optimization of command parameters by sliding speed of an MSAP" Université of Tlemcen, Master's Memoir, 2020/2021.

[40] I. Deghboudj, "command of non-linear systems by means of a higher-order sliding mode" Université Constantine, Mémoire de Magister, 2013.